| OF |
AD
A055998

END
DATE
FILMED
9 -78
DDC

1.0

4.5
5.0
5.6

2.8   2.5

3.2   2.2

3.6

4.0   2.0

1.1

1.8

1.25   1.4   1.6

MICROCOPY RESOLUTION TEST CHART
NATIONAL BUREAU OF STANDARDS-1963-A

LEVEL-II   ARO-12728.3-P

(12)

(14) UILU-ENG-78-2543

AD A055998

(6) OPTICALLY PUMPED FAR INFRARED LASERS.

(9) Final Report for the Period 1 Mar 75 - 28 Feb 78
March 1, 1975 - February 28, 1978

by

(10) T. A. /DeTemple and P. D. /Coleman

(11) June 1978   (12) 57 p.

Prepared for
U.S. Army Research Office
P.O. Box 12211
Research Triangle Park, NC 27709

4

DAHC 04-75-G-0099

Prepared by
Electro-Physics Laboratory
Department of Electrical Engineering
Engineering Experiment Station
University of Illinois
Urbana, Illinois 61801

(15) DAHC04-75-G-0099

(18) ARO   (19) 12728.3-P

403 714 78 07 03 055   JOB

The findings in this report are not to be
construed as an official Department of the
Army position, unless so designated by
other authorized documents.

REPORT DOCUMENTATION PAGE		READ INSTRUCTIONS BEFORE COMPLETING FORM
1. REPORT NUMBER	2. GOVT ACCESSION NO.	3. RECIPIENT'S CATALOG NUMBER
4. TITLE (and Subtitle) OPTICALLY PUMPED FAR INFRARED LASERS		5. TYPE OF REPORT & PERIOD COVERED Final 3-1-75/2-28-78
		6. PERFORMING ORG. REPORT NUMBER ~~UILU-ENG-78-2543~~
7. AUTHOR(s) T.A. DeTemple and P.D. Coleman		8. CONTRACT OR GRANT NUMBER(s) DAHC 04-75-G-0099
9. PERFORMING ORGANIZATION NAME AND ADDRESS Department of Electrical Engineering University of Illinois Urbana, Illinois 61801		10. PROGRAM ELEMENT, PROJECT, TASK AREA & WORK UNIT NUMBERS
11. CONTROLLING OFFICE NAME AND ADDRESS U. S. Army Research Office Post Office Box 12211 Research Triangle Park, NC 27709		12. REPORT DATE June 1978
		13. NUMBER OF PAGES 54
14. MONITORING AGENCY NAME & ADDRESS(if different from Controlling Office)		15. SECURITY CLASS. (of this report) Unclassified
		15a. DECLASSIFICATION/DOWNGRADING SCHEDULE NA

16. DISTRIBUTION STATEMENT (of this Report)

Approved for public release; distribution unlimited.

17. DISTRIBUTION STATEMENT (of the abstract entered in Block 20, if different from Report)

NA

18. SUPPLEMENTARY NOTES

The findings in this report are not to be construed as an official Department of the Army position, unless so designated by other authorized documents.

19. KEY WORDS (Continue on reverse side if necessary and identify by block number)

Far infrared lasers
Superradiance
Stimulated Raman emission

Micrometers

20. ABSTRACT (Continue on reverse side if necessary and identify by block number)

Experiments and theory regarding the emission processes in optically pumped far infrared laser sources are reported. Super-radiance from CH_3F at 496 μm in the homogeneously broadened regime has been identified for the first time. Stimulated Raman emission on pure rotational transitions in D_2O at 50 μm and 66 μm has also been identified for the first time. Generally good

DD FORM 1473 EDITION OF 1 NOV 65 IS OBSOLETE
1 JAN 73

agreement between experiments and a Maxwell-Bloch approach was obtained for the superradiance study, and good qualitative agreement between experiments and a Maxwell-density matrix approach using three waves interacting in a four-level system was noted for the Raman study; both implying that the processes are now reasonably well characterized and understood.

TABLE OF CONTENTS

OPTICALLY PUMPED FAR INFRARED LASERS

I. OVERVIEW

This report summarizes the research performed under Grant
DAHC 04-75-G-0099 during the period 1 March 1975 to 28 Feb-
ruary 1978. The basic research goals were quite simple: the
study of fundamental processes associated with the optical
pumping technique used to generate far-infrared radiation.
Two specific areas addressed in detail are superradiance and
stimulated Raman emission, both identified and partially
characterized during the course of this study.

II. SUPERRADIANCE

A. Introduction

The concept of superradiance, as originally presented
by Dicke,[1] is that of the collective spontaneous decay of an
ensemble of two-level atoms prepared in a superposition state.
The resultant emission intensity is proportional to the square
of N, the number of atoms, and is emitted in a delayed pulse
whose delay and width are both inversely proportional to N.
The theory has evolved to treat extended media,[2] complete in-
version,[3] swept excitation,[4] and various other effects such as
relaxation and degeneracy.[5] At the time of the proposal, one
experimental observation of superradiance had been made,[6] and

the question was whether our observations on methyl fluoride were of the same effect and what modifications would have to be made in the existing theory[2] to allow a comparison.

The objectives of the proposal were several; and with one exception, they have all been fulfilled at least as well as we had hoped. The details of the superradiant pulse evolution have been studied and are described in the next section. The scaling behavior of the superradiant emission with cross sectional area A, has been found to be intermediate between that of the disk and needle cases,[2] that is, the intensity varies more rapidly than A but more slowly than A^2 (see Appendix I); with length, L, the variation ($\sim$ as L^3) is faster than that predicted, as is discussed in the next section. Seeding of the sample to determine the initial condition (initial Bloch vector tipping angle) of the Maxwell-Bloch theory[5] has not been done, because reproducible far infrared pulses of intensity approximately 10^{-19} W/cm^2 would be required. The theory of Ref. 5, developed independently by us in a similar version, appears to give not only the qualitative features of the superradiant emission, but also a quantitative fit to our results over a range of cell length and CH_3F pressure, using only one free parameter; this is discussed in more detail in the next section. This analysis has given an indication of the conditions under which superradiance may evolve; in particular, it appears

that population decay and dephasing effects (represented by $T_2=T_1$) are not as serious as was first thought. And, finally, an efficient pulsed far infrared source (15% photon conversion efficiency) has been realized; the efficiency is related only to the finite delay and finite pump pulse width, but the conditions for superradiant emission limit the intensity to less than a kilowatt at the present time.

Contributions in amplification of, or in addition to, those proposed have taken place in several different areas, both theoretical and experimental. One of these was the extension of the theory of the propagationless case[7] to include, phenomenologically, collisional dephasing and energy loss $(T_2 \& T_1)$ and to investigate the importance of these relative to Doppler dephasing; it was found that the latter is the less serious case. A search was made for candidate transitions; several far-infrared (FIR) possibilities (pumpable by a CO_2 TEA laser) were found (see Ref. 8), and we identified alkali metal vapor transitions on which subsequent observations of superradiance were made.[9,10,11] The apparatus has been modified to allow for shorter, more stable pump pulses, to further reduce feedback and symmetrize the sample cell with respect to forward- and backward-propagating waves, and to allow sensitive detection of the superradiant pulses on a nanosecond time scale. An analytical solution has been found for the small-area pulse

case and agrees with computer calculations in the proper limits, and an empirical expression for the dependence of the pulse parameters on cell length has been derived from computer solution of the equations of Ref. 4. The effects of varying cross-sectional area, length, and pump duration have been studied experimentally and theoretically, and the pulse shape observed in detail; in addition, the transitions from superradiance to swept-gain superradiance and from homogeneous to Doppler broadening have been observed and studied.

B. Summary of Research

Earlier results have been reported at several conferences (Refs. 8,12; Appendix I); the latest results have been reported at the Tenth International Quantum Electronics Conference, Atlanta, May 29-June 1, 1978, paper T-4, and are being prepared for publication. These results will be summarized here, and general conclusions will be drawn in the next section.

The apparatus is essentially the same as that shown in Fig. 2 of Appendix I, although certain changes have been made. The mode quality of the CO_2 TEA laser has been improved by increasing the inner diameter of the intracavity gain cell, and the output energy has been increased threefold, allowing the pump pulse to be truncated to a width (FWHM) of 15 nsec with a peak power still approximately 1 MW. This allows even higher pressures to be reached before overlap of the pump and FIR

pulses occurs. The pump pulse is now weakly focused by a long-radius mirror into the FIR cell so that it may transverse the maximum length of cell allowed by laboratory dimensions (10.2 m) without expanding appreciably. In addition, the FIR cell has been made symmetric by the mounting of a dielectric-coated silicon "input coupler" at the far end of the cell, reducing feedback even more, allowing full detection of the pump, and eliminating the need for external separation of the pulses. This arrangement allows for the extension of the range of data to even lower pressures, and allows the measurement of the delay of the backward wave. The Si:P detector has been more carefully calibrated and has been operated at lower bias to decrease its response time to about 2 ns (at the expense of sensitivity) in order to follow faithfully the time behavior of the FIR pulses from the longest samples.

Typical pulses are shown in Fig. 1, where the qualitative dependences of the intensity, pulse width, and delay (measured from pump cutoff) on pressure and cell length can be seen. In Fig. 1c, the fluctuations in the FIR pulses are also evident (the lowest FIR pulse is due to the unusual fluctuation in the pump).

Measurements of the delay, width, and intensity of the superradiant pulses were made as a function of CH_3F pressure at several cell lengths: 168, 229, 351, 473, 656, 838, and
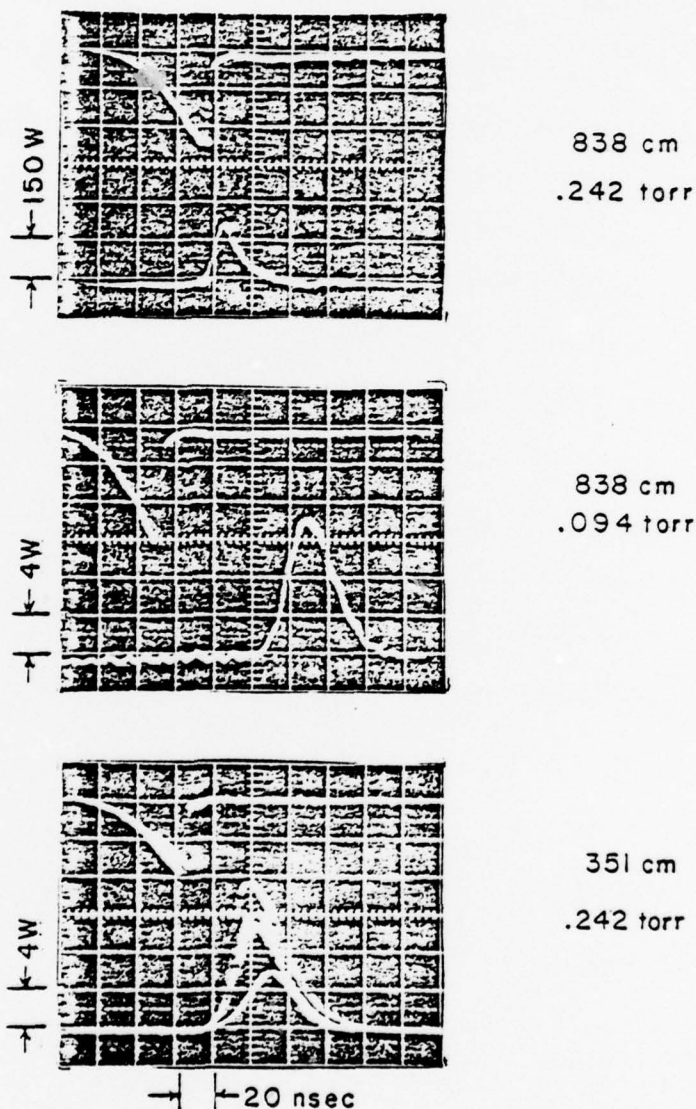
Fig. 1.   Typical pulses showing the qualitative effects of varying
pressure for a given cell length and of varying cell
length at constant pressure. The upper pulse is the CO_2
pump, showing the rapid cutoff; a) nearly-overlapping
pulses; vertical scale is 150 W/div (FIR pulse only),
horizontal scale 20 nsec/div., b) well-separated pulses
at a lower pressure; note change in vertical scale to
4 W/div., c) five pulses at .242 torr in a shorter cell,
showing a somewhat larger-than-normal range of fluctuation.

1021 cm; this was done for both the forward- and backward-going pulses. Since it is expected that the delay and width should vary with pressure as p^{-1}, and the intensity as p^2, the delay and width have been plotted vs p^{-1} and the intensity vs p^2 for the forward-going wave at four cell lengths in Figs. 2, 3, 4, and 5. The delay and width in Fig. 2 are shown with a straight-line fit; the agreement is reasonable. Note the negative delay at infinite pressure ($p^{-1}=0$); this is a result of the finite width of the pump pulse and is the same at all lengths. The intensity dependence is a combination of two straight lines (approximately), one below $p^2 = .01$ torr^2 and a steeper one at higher pressures. Fig. 3 shows the same behavior observed in a 351 cm cell; in all of these plots (Figs. 2-5), the data points represent an average of several pulses. In Fig. 4, at 656 cm, the break in the slope of intensity vs p^2 is seen to correlate with breaks in delay and width vs p^{-1}; this, then, is assumed to be the transition between homogeneous and Doppler broadening, which takes place from 0.10-0.04 torr. This behavior is even more evident in Fig. 5.

In Fig. 6 is shown the dependence of the pulse parameters on length for two pressures. Both delay and width show a decrease and appear to be approaching nonzero values; the shortest delays are approximately equal to T_2, and all but the longest pulse widths are less than T_2. In spite of this,
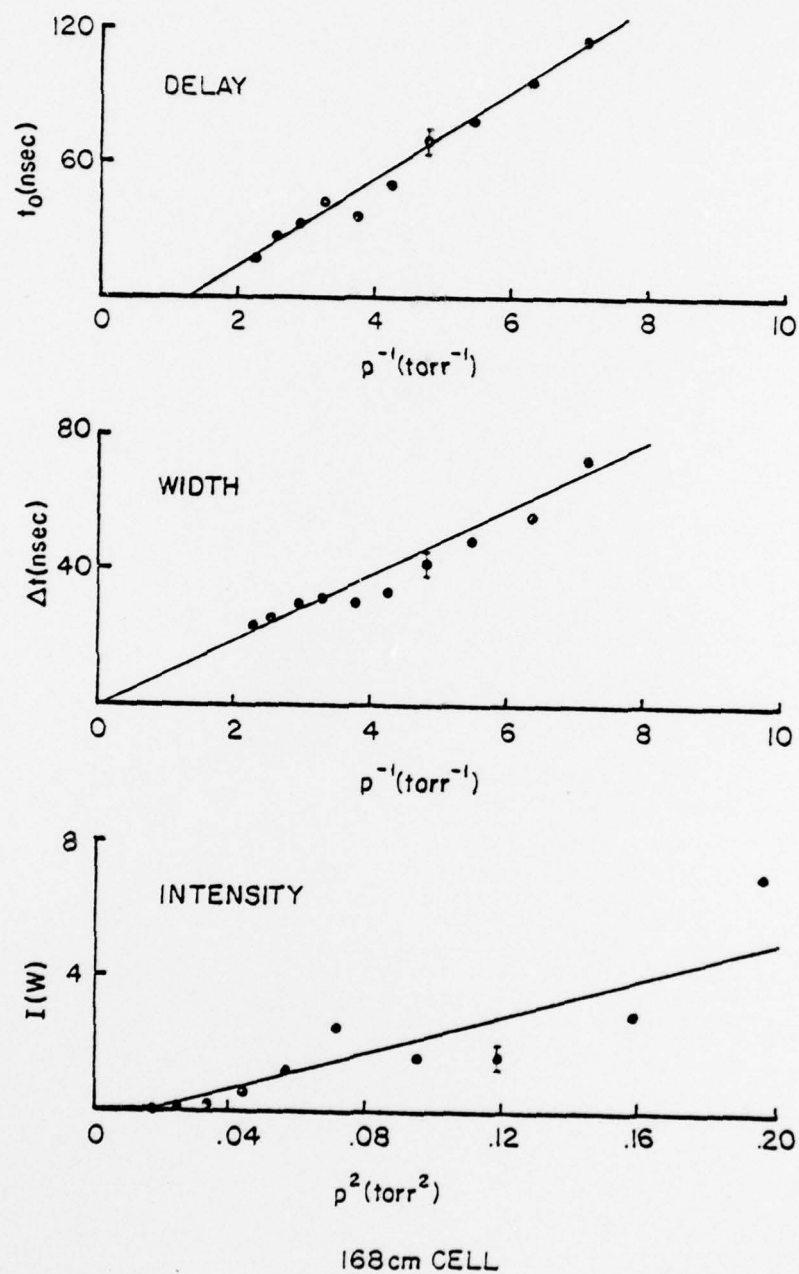
168 cm CELL

Fig. 2. Delay (measured from pump cutoff to FIR peak) vs.
inverse pressure, pulse width vs. inverse pressure,
and pulse intensity vs. pressure squared, for a cell
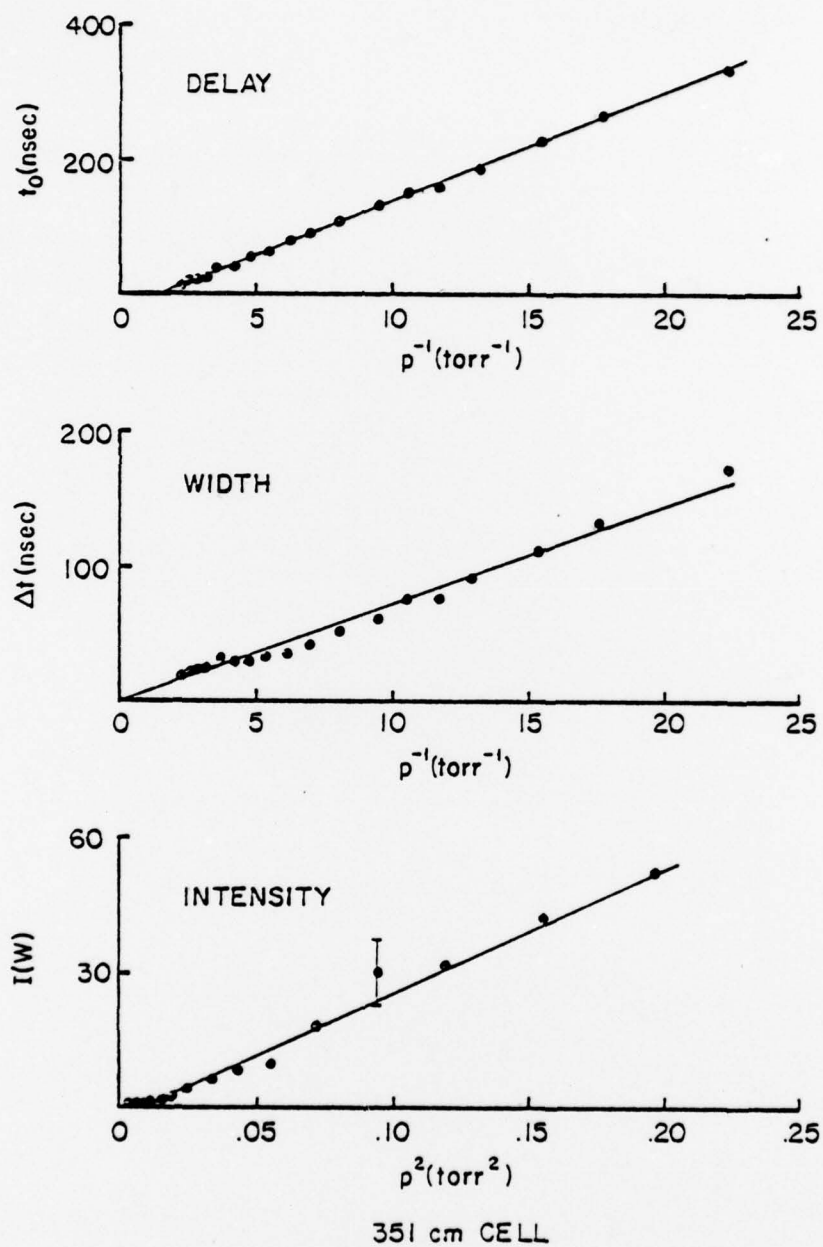length of 168 cm. The intercept of the delay at
$p^{-1} = 0$ is -23 nsec.

Fig. 3. Delay and pulse width vs. inverse pressure, and intensity vs. pressure squared for a 351 cm cell.
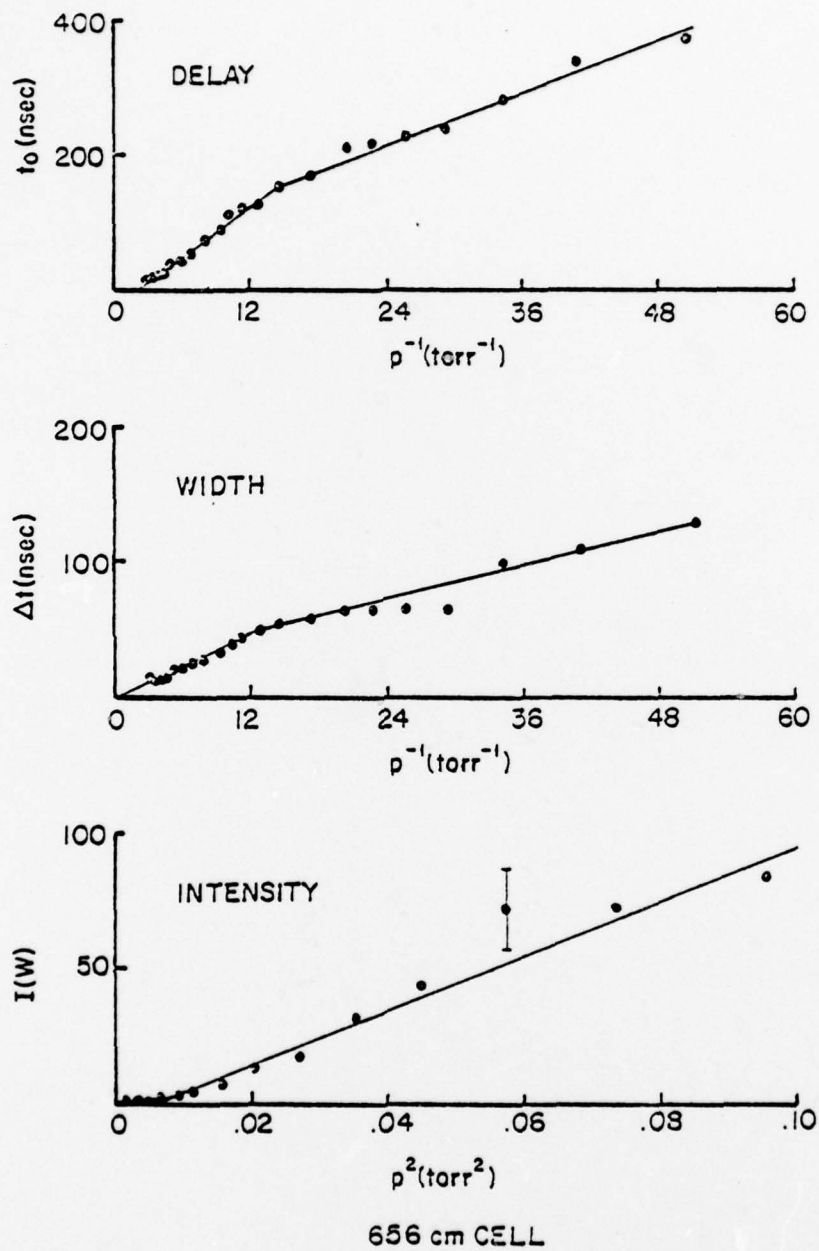
Fig. 4. Delay and pulsewidth vs. inverse pressure, and
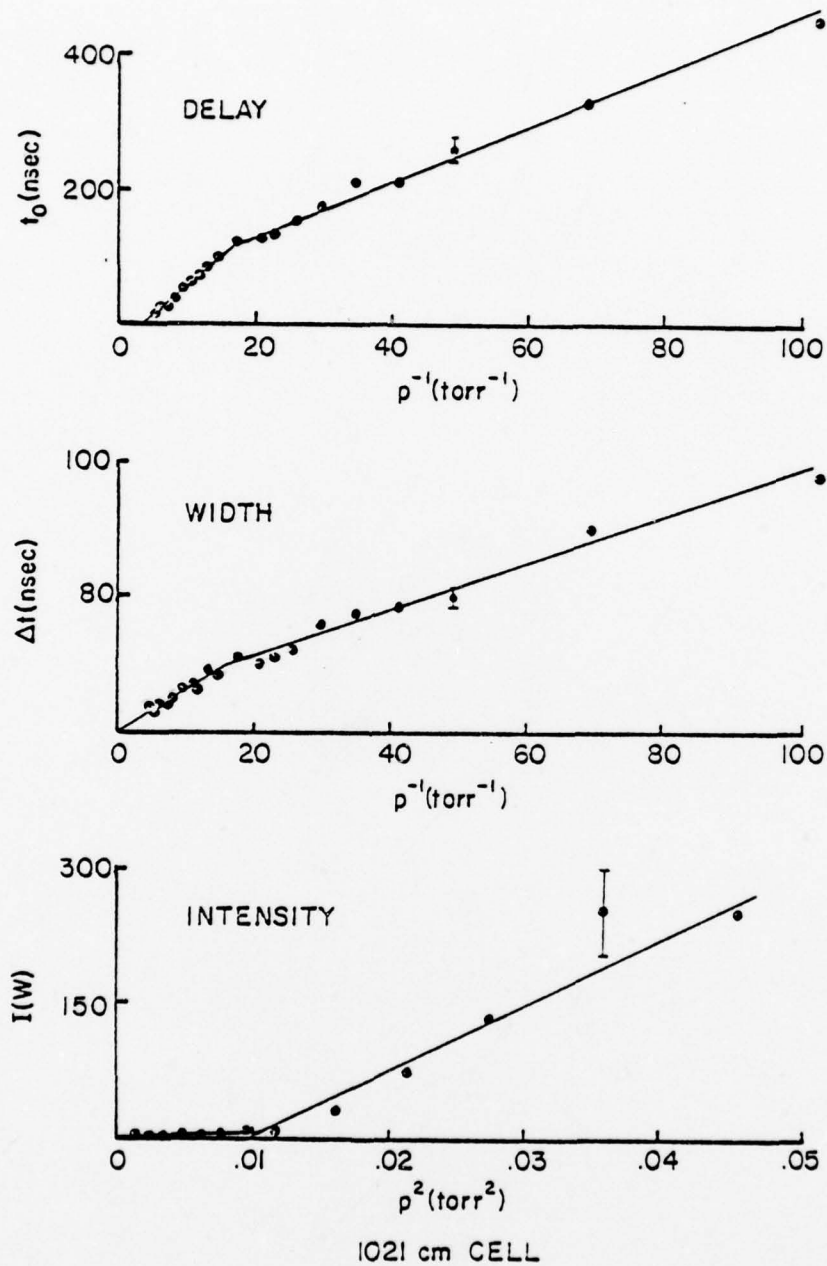intensity vs. pressure squared for a 656 cm cell.

Fig. 5. Delay and pulse width vs. inverse pressure, and
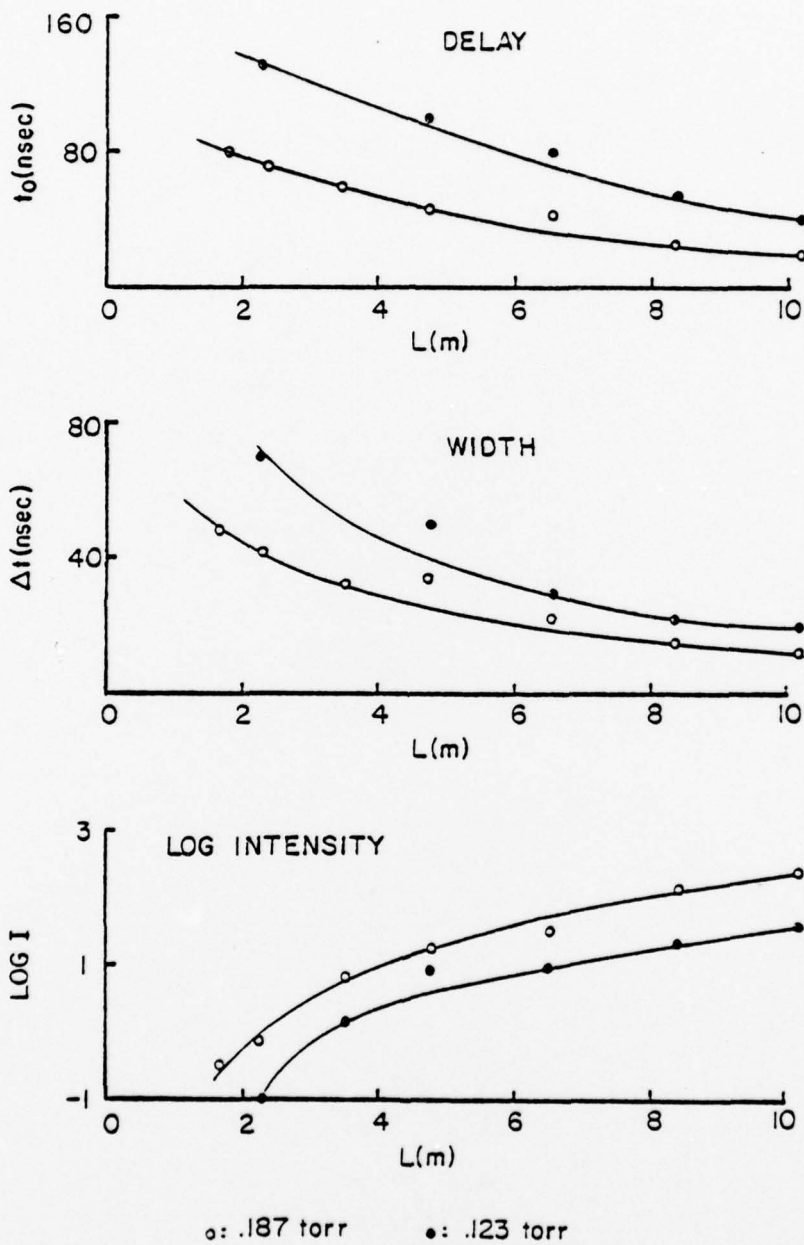intensity vs. pressure squared for a 1021 cm cell.

Fig. 6. Delay, width and log intensity vs. L for two pressures, .187 torr and .123 torr.

ringing was never observed in the FIR pulses. The intensity shows an increase approximately as L^3 over this range of lengths. Fig. 7 shows the ratio of the forward FIR intensity to the backward intensity plotted vs p for fixed L and vs L for fixed p; it is seen that the characteristic of the emission goes from that of Dicke superradiance ($R \approx 1$) to that of swept-gain superradiance ($R \gg 1$) as p increases past .10 torr and as L increases past 5 m. This is supported by the delay and width variation with L; both go as a larger negative power of L for $L > 5m$.

Fig. 8a shows an example of the fit that can be obtained with the Maxwell-Bloch equations with a fluctuating-phase input field to simulate the initial tipping angle due to spontaneous and blackbody emission. Here the pump pulse is assumed to be saturating and the loss is calculated as that of a Gaussian beam.[5] The initial tipping angle, θ_0, is the only free parameter, and by setting $\theta_0 = \dfrac{c(L)}{\sqrt{N}}$, the results for pressures ranging over the homogeneously broadened regime are fit fairly well for the shorter cell lengths (c depends only on L, not p, and is on the order of 1). The arrows in Fig. 8a represent the range of fluctuation predicted numerically for the intensity and delay. Figs. 8b and 8c show the effect of varying the loss and the tipping angle, respectively. The dashed line in all three represents the experimental result. It is
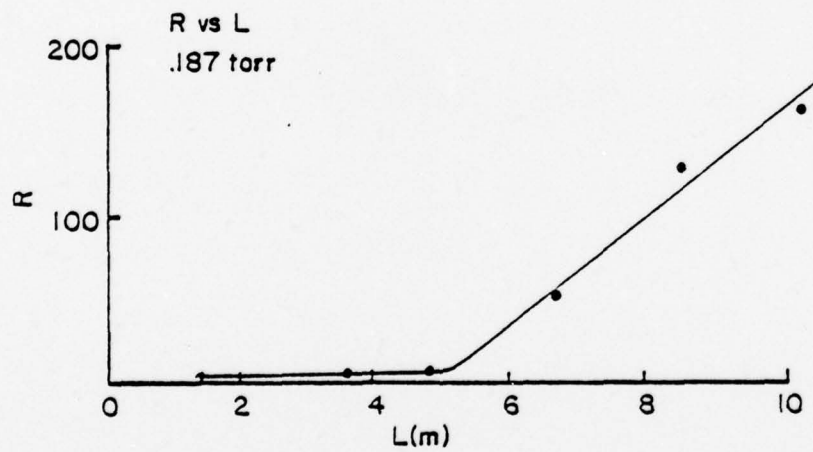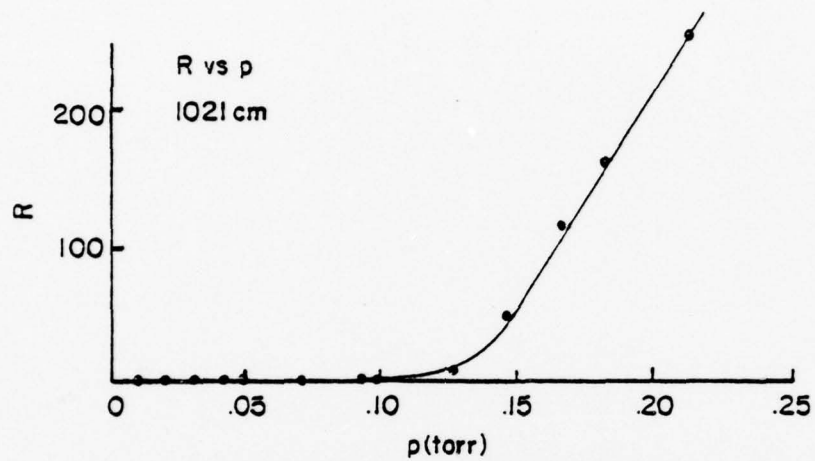
Fig. 7. The dependence of the ratio of forward intensity to backward intensity, R, vs. p at a fixed length (1021 cm), and vs. L at a fixed pressure (.187 torr).

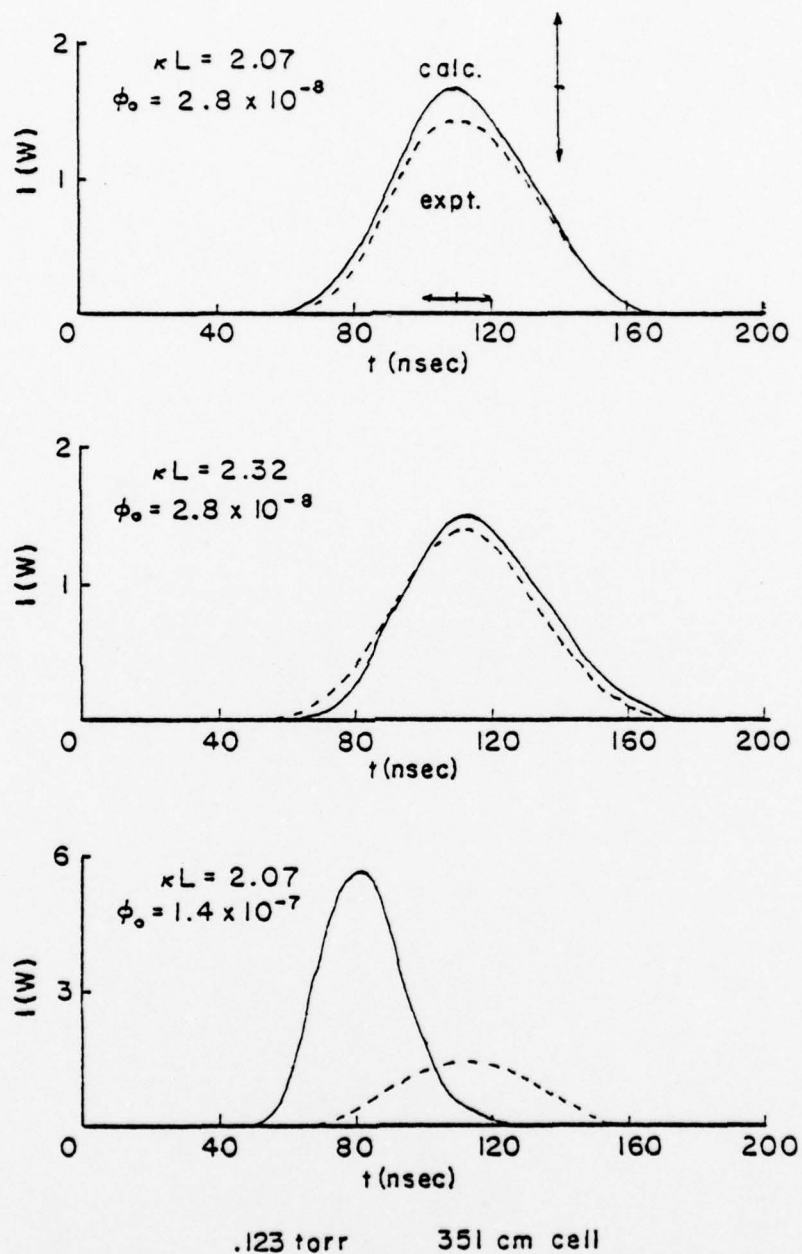Fig. 8. Comparison of calculated (solid lines) pulses to experimental (dashed lines) pulses, showing sensitivity of the calculation to variations in initial tipping angle (θ_0) and loss (kL). a) Best fit found by calculating kL and varying θ_0. The arrows show the range of fluctuation in intensity and delay predicted. b) Effect of varying kL slightly. c) Effect of a variation in θ_0; note vertical scale change.

found that a fit can be obtained for a small change in k by changing θ_0; in other words, the fit is not sufficient to determine the absolute value or perhaps even the functional form of θ_0 because k is merely an estimate. It is also found that the fit is not as good (quantitatively) for long cells or for the backward wave, for reasons which will be discussed in the next section.

C. Conclusions

It is seen that agreement between theory and experiment is fairly good except for the longest cell length and for the backward wave. The agreement is improved by including a finite-width pump pulse, which is effectively an intermediate case between simultaneous (e.g., transverse) and swept (delta-function) excitation. It also appears from initial computations that the inclusion of degeneracy for the FIR transition does not have an appreciable effect; it may be possible, however, that the pump transition degeneracy may, when included, have an effect, and that the combination of this with the finite pump pulse width may have an even greater effect. Other things which may have to be included in the model are coherent pump effects, Doppler broadening of the FIR transition, and transverse variation of the pump resulting in lensing effects for the FIR. Far infrared pulses as short as 12 nsec and as

intense as 250 W have been produced in a superradiant manner
(no pulse overlap between pump and FIR). This is limited, at
present, by the finite width of the pump pulse, and possibly
by other factors such as degeneracy and transverse effects.

The major contribution of this work has been that super-
radiant emission has been observed in the homogeneously broad-
ened regime for the first time, and that ringing has been ab-
sent even when the delay is less than T_2. The dependence of
the delay, pulse width, and intensity has been investigated
as a function of pressure, cell length, and cross-sectional
area and the scaling behavior found to be intermediate between
the disk and needle limits for shorter cells. The expected de-
pendences on pressure have been found, with the additional
feature of the transition from homogeneous to Doppler broad-
ening being reflected as a change of slope in all three cases.
In addition, the effect of a finite pump width has been seen
in a negative intercept for the delay at $p^{-1}=0$; this inter-
cept is approximately 1.5 times the FWHM of the pump pulse,
which indicates that only the initial part of the pump is
necessary to prepare the state of FIR inversion. And finally,
the observation of the transition from Dicke superradiance to
swept-gain superradiance first reported in Ref. 12 has been
corroborated and amplified.

III.   STIMULATED RAMAN EMISSION

A.   Introduction

D$_2$O vapor, optically pumped with a CO$_2$ TEA laser, has been under study regarding the nature of far-infrared (FIR) emission associated with pure rotational transitions. In the course of preliminary research, several features of particular interst emerged which have been subjects of further investigation. The 50 μm and 66 μm emission lines, pumped with the 9.66 μm P(32) CO$_2$ line, have been shown to constitute stimulated Raman emission and to lie ∿ 2 GHz from corresponding ground state and ν$_2$ rotational transitions. This is to be compared with the measured 1.1 GHz detuning of the CO$_2$ pump from the relevant 000 6$_{61}$,6$_{60}$ → 010 5$_{50}$,5$_{51}$ IR absorption doublet (energy level notation is J$_{K-1,K+1}$).[13] Several other D$_2$O transition detunings from CO$_2$ pump lines were measured as summarized in Table II of Appendix II.

Various emission line assignments were made on the basis of recent spectroscopy of the ν$_2$ band of D$_2$O.[14] The scheme of the P(32) pump line and observed emission lines is shown in Fig. 9. Neglecting the weak 83 μm cascade transition and the 116 μm line, the system is comprised of three radiation fields present on the dipole-allowed transitions connecting four molecular levels. We have undertaken the analysis of such a system in the homogeneously broadened regime by means of a
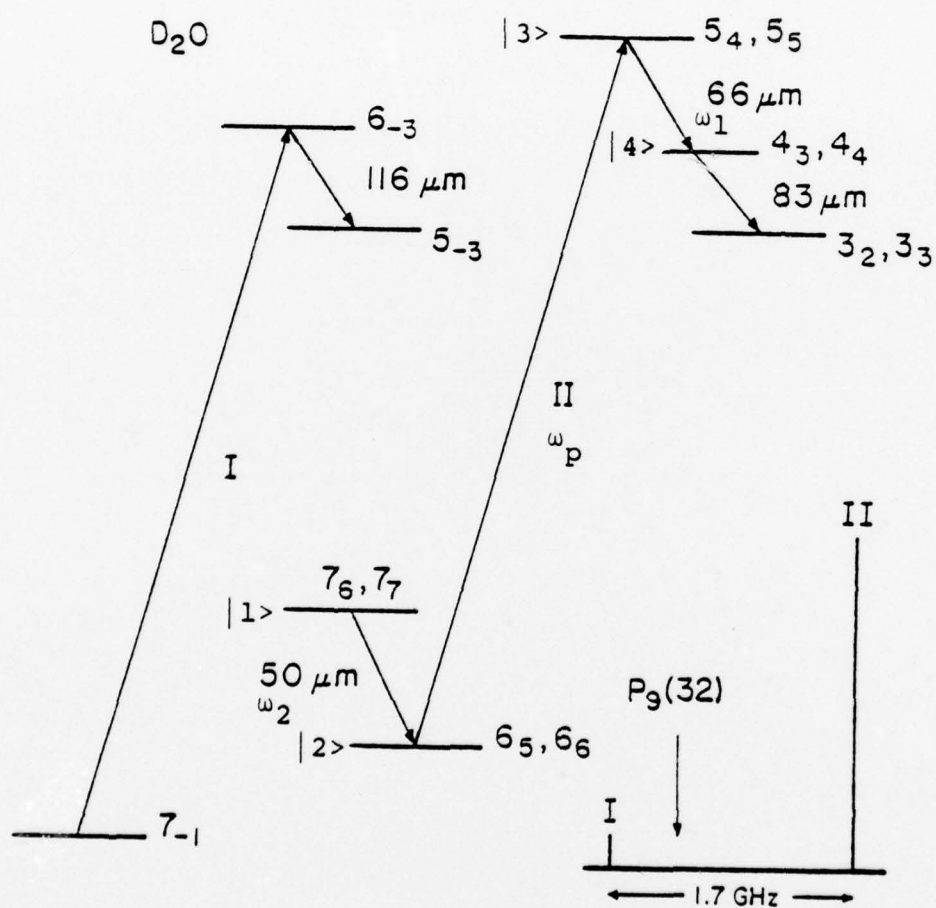
Fig. 9. Partial D_2O energy level diagram near the $P_9(32)$ laser line. Insert shows the detailed absorption spectra based on tunable diode laser spectroscopy of Ref. 13.

quasi-static density matrix formalism, and have derived exact algebraic expressions for wave gain profiles which point to nonlinear mechanisms of wave coupling. This analysis has been incorporated into a computer program in which the evolution of the 66 μm and 50 μm emission in a single-pass system is modeled.

B. Analysis

The four-level density matrix analysis applied to the D_2O system indicates that two-photon processes such as optically pumped lasing and stimulated Raman emission are significantly modified by an interaction with an intense third radiation field. The system of coupled density matrix equations has been solved quasi-statically (in the $t \gg T_2$ limit), neglecting off-resonant and transient terms in favor of terms with small resonance denominators. Albebraically exact expressions have thus been derived for the off-diagonal elements of the density matrix in terms of arbitrary field intensities, population differences, detunings, and phenomenological dephasing and damping processes. Field gains can then be cast in a form in which terms are grouped by population differences and contributions to the net gain by one-,two-, and three-photon processes are thereby elucidated.

In the level configuration depicted in Fig. 9, applicable to the D_2O system, the ε_1 gain assumes the form:

$$G_1 \propto \alpha_1(n_3-n_4) + \omega_p^2 \alpha_2(n_2-n_4) + \omega_p^2\omega_2\alpha_3(n_1-n_4)$$

where (n_i-n_j) is the population difference between levels i and j, α_i are coupling factors peaked, respectively, near i-photon resonances, and ω_i are the Rabi frequencies. The α_i are field-dependent, and account for relative polarizations of the interacting fields as well as AC Stark shifts. Exact field intensity-dependent expressions have been derived for the AC Stark shifts and i-photon linewidths. An appropriate summation over sublevels incorporates the effect of the M-degeneracy of the rotational levels, lifted in the presence of intense optical fields.

In the D_2O system of Fig. 9, the 50 μm ground state transition cannot be inverted on a quasi-steady-state basis and laser loss is predicted on resonance. However a two-photon (SRE) gain multiplier, α_2, plotted in Fig. 10 as a function of frequency and 66 μm field intensity at a characteristic D_2O pressure and pump intensity, yields a net gain off-resonance under population conditions characteristic of a saturated 66 μm SRE process. This partially accounts for the observed delayed onset of the 50 μm signal (see Fig. 3 of Appendix II).

C. Experiment

The system on which our optically pumped D_2O research has been carried out is essentially that described in Appendix
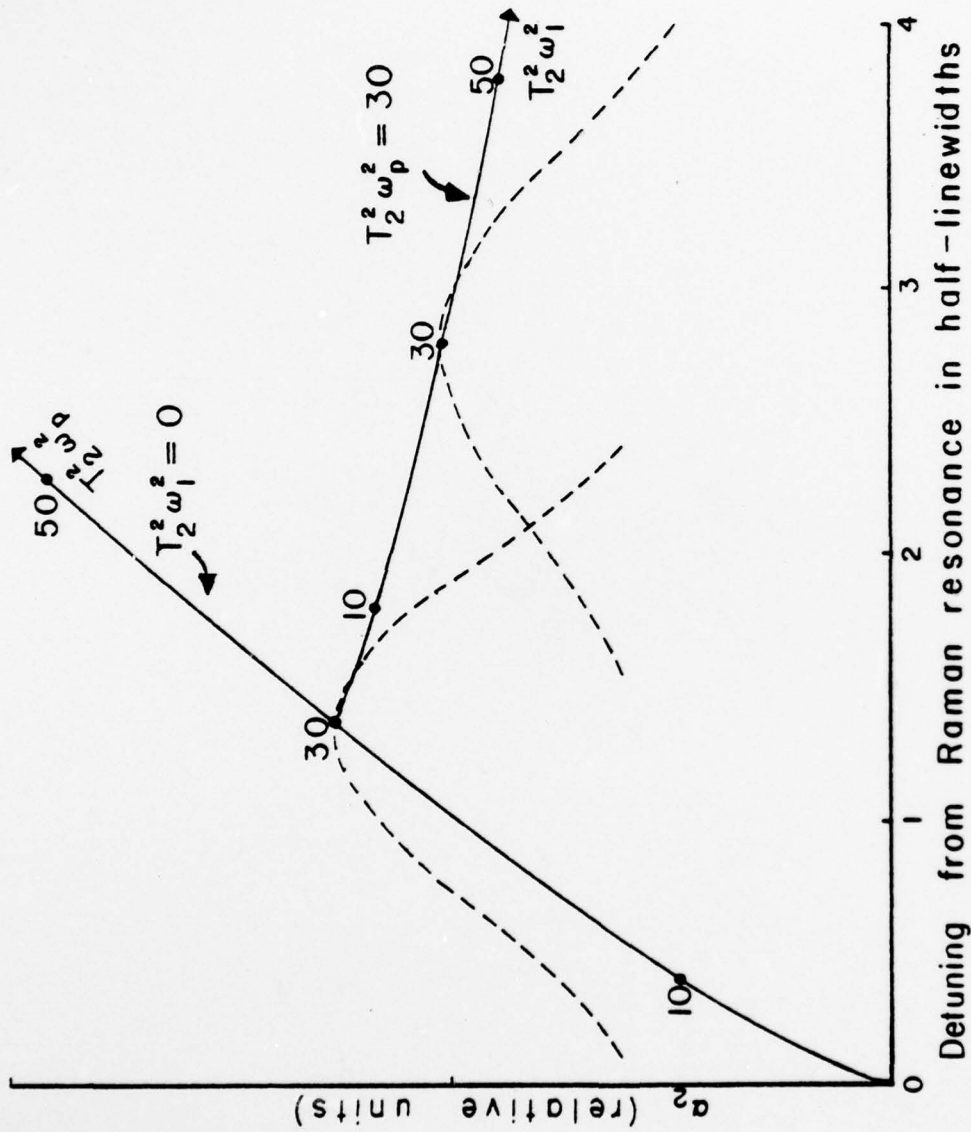
Fig. 10. Loci of maximum α_2 and detuning from Raman resonance at maximum α_2 pertaining to the 50 μm D$_2$O line, at a pump detuning of 1.1 GHz and a D$_2$O pressure of 2.2 torr. For a FWHM linewidth of 40 MHz/torr, $T_2^2 \omega_p^2 = 50$ corresponds to a pump intensity of 822 kW/cm^2 while $T_2^2 \omega_l^2 = 50$ corresponds to a 66 μm signal intensity of 2.9 kW/cm^2. Two gain profile segments illustrate the line broadening influence of the 66 μm signal.

22

II. Detunings of pump and FIR fields were determined on the basis of pressure dependence of absorption in D_2O as described there. Subsequent modifications have included improvement of the TEA laser transverse beam quality and stability (by geometrical modifications of the CW amplifier section), and elimination of the Au-coated back reflector and all surfaces normal to the FIR beam to ensure single-pass operation. A cell containing cyclopropane at variable pressure in line with the pump beam allows continuous variation of pump intensity from shot to shot. Net 66 μm pulse energies and their shot-to-shot fluctuations have been measured as functions of cell length, pressure, and pump intensity in the single-pass configuration.

At a pump energy of 72 mJ/pulse, FIR energy fluctuations are characteristic of saturation of the 66 μm SRE process within a length ∿ 2.5 m, assuming an incoherent blackbody source at the input end of the cell.[15] Gain and threshold estimates derived from these data are reasonable within the context of our theoretical understanding of the system. Real time measurements will allow detailed comparison with the single-pass propagational model we have developed.

One further feature predicted by our analysis is currently under study. As the FIR gain profile is a function of field intensities, a chirp in the frequency of the emitted FIR pulse is to be expected as the pump pulse rises from FIR threshold

to its peak value. This is being studied by a time-resolved interferometric technique with the major goal of identifying the magnitude of the chirp and hence the 'start' condition for the emission.

D. Conclusions

Inroads have been made into the understanding of FIR emission by a molecular system optically pumped off-resonance in the infrared. The SRE mechanism whereby the strong 66 μm and the 50 μm lines are generated in D_2O has been identified for the first time. Research into the precise field and molecular population dynamics is well underway with implications for a variety of other configurations of coupled waves in gaseous systems.

REFERENCES

1. R.H. Dicke, Phys. Rev. 93, 99 (1954).

2. N.E. Rehler and J.H. Eberly, Phys. Rev. A. 3, 1735 (1971).

3. R. Bonifacio and L.A. Lugiato, Phys. Rev. A. 11, 1507 (1975).

4. R. Bonifacio, F.A. Hopf, P. Meystere, and M.O. Scully, Phys. Rev. A. 12, 2568 (1975).

5. J.C. MacGillivray and M.S. Feld, Phys. Rev. A. 14, 1169 (1976).

6. N. Skribanowitz, I.P. Herman, J.C. MacGillivray, and M.S. Feld, Phys. Rev. Lett. 30, 309 (1973).

7. R. Jodoin and L. Mandel, Phys. Rev. A. 9, 873 (1974).

8. A.T. Rosenberger, S.J. Petuchowski, and T.A. DeTemple, in Cooperative Effects in Matter and Radiation, C.M. Bowden, D.W. Howgate, and H.R. Robl, eds. (Plenum, N.Y., 1977), p. 15.

9. M. Gross, C. Fabre, P. Pillet, and S. Haroche, Phys. Rev. Lett. 36, 1035 (1976).

10. Q.H.F. Vrehen, H.M.J. Hikspoors, and H.M. Gibbs, Phys. Rev. Lett. 38, 764 (1977), and Q.H.F. Vrehen, in Cooperative Effects in Matter and Radiation, C.M. Bowden, D.W. Howgate, and H.R. Robl, eds. (Plenum, N.Y., 1977), p. 79.

11. A. Flusberg, T. Mossberg, and S. R. Hartmann, Phys. Lett. 58A, 373 (1976), and in Cooperative Effects in Matter and Radiation, C.M. Bowden, D.W. Howgate, and H.R. Robl, eds. (Plenum, N.Y., 1977), p. 37.

12. J.J. Ehrlich, C.M. Bowden, D.W. Howgate, S. H. Lenigh, A.T. Rosenberger, and T.A. DeTemple, to be published in the Proceedings of the Fourth Rochester Conference on Coherence and Quantum Optics, L. Mandel and E. Wolf, eds. (Plenum, N.Y., 1978).

13. T.L. Worchesky, K.J. Ritter, J.P. Sattler, W.A. Riessler, Opt. Lett. 2, 70 (1978).

14. C.L. Lin and S.H. Shaw, J. Mol. Spec. 66, 441-447 (1977).

15. S.A. Akhmanov, Yu. E. D'yakov, and L.D. Pavlov, Sov. Phys. JETP, 39, 249 (1974).

IV. PUBLICATIONS

1. "Fir Absorption Determination of Transient Electron Densities in High-Pressure Ionizer-Sustainer Lasers", L.A. Newman, M.R. Schubert, and T.A. DeTemple, J. Appl. Phys., <u>47</u>, p. 4904 (1976).

2. "Stimulated Raman Emission in Infrared Excited Gases", S.J. Petuchowski, A.T. Rosenberger, and T.A. DeTemple, IEEE J. Quan. Elec., <u>QE-13</u>, p. 476 (1977).

3. "Diffraction Limited CW Optically Pumped Lasers", M. Schubert, M. Durschlag, and T.A. DeTemple, IEEE J. Quan. Elec., <u>QE-13</u>, p. 455 (1977).

Contributions in Books

1. A.T. Rosenberger, S.J. Petuchowski, and T.A. DeTemple, "Experiments in FIR Superradiance", in <u>Cooperative Effects in Matter and Radiation</u>, ed. by C.M. Bowden, D.W. Howgate, and H. Robl, Plenum: New York (1977), pp. 15-36.

2. A.T. Rosenberger, S.J. Petuchowski, and T.A. DeTemple, "Far Infrared Superradiance in Methyl Fluoride", in <u>Coherence and Quantum Optics IV</u>, ed. by L. Mandel and E. Wolf, Plenum: New York (1978).

3. T.A. DeTemple, "High Power, Pulsed Optically Pumped Lasers and Oscillator Amplifier Systems", in <u>Infrared and Submillimeter Waves, Vol. 1, Sources</u>, ed by K.J. Button, Academic Press: New York (1978).

4. J.J. Ehrlich, C.M. Bowden, D.W. Howgate, S.H. Lehnigk, A.T. Rosenberger, and T.A. DeTemple, "Swept-Gain Superradiance in CO_2 Pumped CH_3F", in <u>Coherence and Quantum Optics IV</u>, ed. by L. Mandel and E. Wolf, Plenum: New York, (1978).

V. SCIENTIFIC PERSONNEL ASSOCIATED WITH GRANT

1. Paul D. Coleman, Principal Investigator

2. Thomas A. DeTemple, Principal Investigator

3. Mark Gimple, M.S. 1976

4. Albert T. Rosenberger, Ph.D. 1978

5. Samuel J. Petuchowski, Ph.D. 1978

APPENDIX I.

FAR-INFRARED SUPERRADIANCE IN METHYL FLUORIDE[*]

A.T. Rosenberger and S.J. Petuchowski
Department of Physics
University of Illinois
Urbana, Illinois 61801

and

T.A. DeTemple
Department of Electrical Engineering
University of Illinois
Urbana, Illinois

Strong superradiant emission at 496 μm from CH_3F optically pumped by a CO_2 TEA laser has been observed in the homogeneously broadened regime. The emitted FIR pulses are asymmetric, exhibit no ringing, and are less than T_2 in width. The FIR pulses are calculated and observed to scale with the geometry of the sample in a fashion intermediate between those of the disk and needle limits. Reasonably good agreement is found between the observations and the predictions of a Maxwell-Bloch treatment in which either the initial tipping angle or a linear loss is considered a free parameter. The FIR emission is observed to vary in character from Dicke superradiance, marked by effectively simultaneous excitation and equal forward and backward intensities, to superradiance more of a swept nature, showing forward-backward asymmetry,

---

although in our short samples, the steady state is not achieved. Qualitative theoretical support for this is provided by bidirectional and propagationless Maxwell-Bloch models.

I. Introduction

The cooperative spontaneous emission of radiation, or superradiance,[1] should be observable from initially fully inverted molecular systems which have high gain and are either 1) shorter than a cooperation length,[2] or 2) inverted by means of swept excitation.[3] The emission from an extended cylindrical sample should occur as delayed pulses, the intensity, width and delay of which depend on the density ρ of excited molecules and on the length L and cross-sectional area A of the sample. The dependence of the delay t_o, width Δt, and peak intensity I of the superradiant pulses on the characteristic time T_s is as follows:

$$t_o \propto T_s, \tag{1}$$

$$\Delta t \propto T_s, \tag{2}$$

$$I \propto N/T_s, \tag{3}$$

where $T_s \equiv 3\tau_N$ and[4]

$$\tau_N = T_{sp}/\mu N \tag{4}$$

Here T_{sp} is the spontaneous lifetime, $N = \rho AL$ is the number of cooperating molecules, and μ is a wavelength- and geometry-

dependent shape factor:[4]

$$\mu = 3\lambda^2/8\pi A, \qquad (F \gg 1; \text{ disk}) \qquad (5)$$

$$\mu = 3\lambda/8L, \qquad (F \ll 1; \text{ needle}) \qquad (6)$$

where the two expressions for μ apply in the limits of large and small Fresnel number $F \equiv 2A/\lambda L$. This implies qualitatively different geometrical dependences of the pulse characteristics at constant density in the large -F and small -F limits:

	disk	needle
$t_o \propto$	L^{-1}	A^{-1}
$\Delta t \propto$	L^{-1}	A^{-1}
$I \propto$	AL^2	A^2L

For a system of Fresnel number of order one, an intermediate geometrical behavior might be expected.

The far infrared should be a regime well suited to the observation of superradiance, because the radiative lifetimes of rotational transitions are long, the gains on these transitions can be high, and the possibility of swept excitation by optical pumping exists. The first observation of super-radiance, in fact, took place on FIR rotational transitions in HF,[5] and the present work on CH_3F is, in a sense, its complement. In the pressure range of interest, the FIR emission from CH_3F is homogeneously broadened. In spite of this, the

superradiant pulses extract a large fraction of the energy
available at the time of emission, and so we claim that the
process involved is more correctly labeled "strong super-
radiance" than "limited superradiance."[7] As can be seen
from Table I, the conditions[7] for "strong superradiance" are
satisfied:

$$T_s \ll T_2, \tag{7}$$

$$\alpha_o L \gg |\ln \phi_o|. \tag{8}$$

In addition, $T_1 = T_2$ for the FIR transition, so the analysis
of Ref. 3 for swept-gain superradiance applies, provided that
the pump width is small enough and the sample long enough.

In Table I are defined and listed the various times and
other parameters associated with a particular set of experi-
mental conditions. The experiments and results are described
in Section II, the results are discussed and compared with
theoretical predictions in Section III, and in Section IV the
assumptions of the theory and the implications of the experi-
mental observations are summarized.

II. Experiments

The energy level diagram in Fig. 1 and the experimental
apparatus of Fig. 2 have been described in detail in Ref. 6,
and only the main points of interest will be repeated here.
The pump in Fig. 1 can be preferentially absorbed in either

K (1 or 2) manifold, although K = 2 is more probably domin-
ant because of the larger matrix element. The resultant FIR
emission will be at 496 μm with a 40 MHz frequency difference
between the two possible FIR lines. Rotational (ΔJ) relaxa-
tion yields a 40 MHz/torr homogeneous linewidth and a nonzero
equilibrium population difference. (Table I).

The CO_2 TEA laser in Fig. 2 has been mounted in an Invar
frame for improved stability and emits a single-mode, 120
nsec, 1.2 MW pulse which is truncated, 35 nsec before its
peak, to a width of about 30 nsec.[8] This early cutoff ex-
tends the pressure range in which the pump and FIR pulses do
not temporally overlap. The positions of the absorber and
the detector system may be interchanged to allow observation
of FIR emission in the direction opposite that of the propaga-
tion of the pump.

The cutoff pump pulse and two typical FIR superradiant
pulses are shown in Fig. 3 in synchronous oscilloscope traces.
The low tail on the pump pulse is the result of a slight im-
pedance mismatch between a pulse amplifier and the oscillo-
scope. The FIR pulses are multiple traces to show shot-to-
shot fluctuations; notice that there is no ringing (ringing
has not been observed on any FIR pulses occurring after cutoff
of the pump) and that the pulses are asymmetric. The quali-
tative pressure (hence density, since the pump is saturating
the IR absorption) dependence is also evident.

The pressure dependence is better shown in Fig. 4, where the data plotted are for a cell 4.7 m long and the lines are least-square fits to the data. The linear variation of delay and width with inverse pressure, and of the average peak intensity with pressure squared, is evident as expected, with slight discrepancies which are qualitatively understood: negative delay at high pressure, and deviation from linear behavior at low pressure. The delay is measured from the cutoff of the pump pulse, so that the finite width of the pump and the onset of swept gain at higher pressure are responsible for the negative delay and deviations in width and intensity.[9] The onset of Doppler broadening below 0.08 torr is thought responsible for the deviation at low pressures. All the pulses are less than T_2 in width.

Comparison of the results for two samples identical except for length is shown in Fig. 5. The qualitative behavior is again the same, but a comparison of the slopes of the least-square linear fits for the two sample lengths shows a behavior intermediate between that of the disk and that of the needle, as given following Eq. (6). The ratio of the intensity of the forward pulse to the intensity of the backward pulse was investigated as a function of pressure, but the results were inconclusive. However, a similar measurement on a 5.9 m sample confirmed the findings of Ref. 9: that the ratio is nearly equal to one at low pressures and becomes

large at higher pressures, when the excitation develops a swept character. One would expect a ratio of one at even higher pressures in a shorter cell.

III. Comparison with Theory

In comparing our results with theory, pump effects. and level degeneracy are neglected and a Maxwell-Bloch approach with an input field fluctuating randomly in phase to simulate spontaneous and black-body emission, much as in Ref. 7, is used. The coupled equations are written in complex form as follows:

$$\frac{\partial}{\partial t} P = - P/T_2 + ER, \tag{9}$$

$$\frac{\partial}{\partial t} R = -(R-R_e)/T_1 - R_e(EP^*), \tag{10}$$

$$\frac{\partial}{\partial x} E = - \kappa E + \alpha P, \tag{11}$$

where $P = - P/\rho\mu_{12}$, $E = \mu_{12}\varepsilon/\hbar$, with μ_{12} being the dipole matrix element between the two FIR levels and P and ε the complex polarization and electric field amplitudes; $R = (N_2-N_1)/N$, the normalized population difference, having an equilibrium value $R_e < 0$. The times T_1 and T_2 are equal for the transition under consideration, $\alpha = (T_s L)^{-1}$ (T_s is here, and in the following, evaluated in the disk limit), and κ is a linear loss to approximate diffraction. It was found that a reasonable fit could be obtained by choosing a credible value

for either κ or ϕ_o and then treating the other as a free parameter. Two representative examples are given in Table II. The observed delay listed in Table II is that measured not from pump cutoff but from the $p^{-1} = 0$ intercept and thus is an overestimation.

The Maxwell-Bloch equations (9)-(11) were modified to treat propagation in both directions, qualitatively confirming the pressure dependence of the forward/backward intensity ratio observed in longer cells and discussed in more detail in Ref. 9. The ratio was calculated to increase with increasing pressure. In the numerical calculations, the asymmetry of the resulting pulses matches that observed, and ringing is predicted only for unphysically large densities or initial tipping angles.[10]

If one assumes no spatial variation in the electric field, and $R_e = 0$, the intensity predicted by Eqs. (9)-(11) has the form

$$I(t) = (\hbar\omega_o\mu N^2/4T_{sp}) \, z^2\text{sech}^2[\beta(1-z) - \alpha], \qquad (12)$$

where $z = \exp(-t/T_2)$, $\beta = T_2/2T_s$, and $\alpha = \ln(2/\phi_o)$. This functional form applies both to the pure Dicke case $L \ll L_c$ and to the steady-state "swept superradiant" case.[3] To see the connection with the latter, note that by using the disk expression for μ, Eq. (5), and replacing L by κ^{-1}, an effective loss length, one may recover the intensity predicted for

the steady-state case with, of course, t being the retarded time.[3] This applies to $L \gg L_c$ and $L \gg \kappa^{-1}$. It is reasonable to seek, then, a fit to this form for the case $L \gtrsim L_c$ if an effective length L_{eff} is used in Eq. (14); this is, in fact, possible, and with the experimental data a fit is found for $L_{eff} \simeq .225 L$. This may be compared with the Maxwell-Bloch prediction that shows spatial variation in the fields and polarization: only the forward $\frac{1}{5}$ to $\frac{1}{4}$ of the sample contributes appreciably to the emission.

IV. Discussion

It has been observed that the FIR emission is sensitive to the exact nature of the shape and frequency of the pump pulse, and this is reflected in a sensitivity of the Maxwell-Bloch model to the specific choice of initial conditions. A prescription for ϕ_o is not yet evident, but it appears to depend more on $N^{-1/2}$ than $(\mu N)^{-1/2}$ in these experiments.[2,3,4] The field losses arrived at in Table II are not consistent with the FIR evolving as a single mode (EH_{11} guided wave loss $< 5 \times 10^{-5} cm^{-1}$) but are comparable to multimode diffraction losses ($\kappa \sim 5 \times 10^{-3} cm^{-1}$), and to absorption of the thermally populated levels in unexcited regions ($\kappa \sim 10^{-3} cm^{-1}$).[11] From these studies, the experimental uncertainties are such that A, ϕ_o, κ and perhaps ρ can be chosen consistently to yield calculated results in good agreement with experiments. Infrared nutation due to the large-area coherent pump also may play a role and should be included in the semiclassical model,

as should the finite width of the pump pulse. A first step to do this has been taken.[9]

To summarize, FIR superradiance in homogeneously broadened CH_3F is "strong" superradiant emission of single asymmetric pulses of width less than T_2, showing the expected dependence on density and exhibiting shot-to-shot fluctuations which are probably due to variation in the pump. The geometrical character of the samples is calculated and observed to be intermediate between the two limits of large and small Fresnel number. The ratio of forward to backward intensities supports the hypothesis of the onset of swept gain in long cells at high pressures. A Maxwell-Bloch approach with either ϕ_o or linear loss κ a free parameter allows a quantitative fit to the observations, and by including bidirectional propagation, the pressure dependence of the forward/backward ratio is qualitatively reproduced for very long cells. The relation to swept excitation is also shown in the effective-length fit of what was called in Ref. 6 the "semiclassical mean-field theory", shown here in Eq. (12). The possibility thus exists in CH_3F of observing superradiance in regimes ranging from $L < L_c$ to the steady-state swept case.

Acknowledgements

References

[1] R.H. Dicke, Phys. Rev. $\underline{93}$, 99 (1954).

[2] R. Bonifacio and L.A. Lugiato, Phys. Rev. A, $\underline{11}$, 1507 (1975).

[3] R. Bonifacio, F.A. Hopf, P. Meystere, and M.O. Scully, Phys. Rev. A, $\underline{12}$, 2568 (1975).

[4] N.E. Rehler and J.H. Eberly, Phys. Rev. A, $\underline{3}$, 1735 (1971).

[5] N. Skribanowitz, I.P. Herman, J.C. MacGillivray, and M.S. Feld, Phys. Rev. Lett. $\underline{30}$, 309 (1973).

[6] A.T. Rosenberger, S.J. Petuchowski, and T.A. DeTemple, in Cooperative Effects in Matter and Radiation, C.M. Bowden, D.W. Howgate, and H.R. Robl, editors (Plenum, N.Y., 1977).

[7] J.C. MacGillivray and M.S. Feld, Phys. Rev. A, $\underline{14}$, 1169 (1976).

[8] E. Yablonovitch, Phys. Rev. A, $\underline{10}$, 1888 (1974); H.S. Kwok and E. Yablonovitch, Appl. Phys. Lett. $\underline{27}$, 583 (1975).

[9] J.J. Ehrlich, C.M. Bowden, D.W. Howgate, S.H. Lehnigk, A.T. Rosenberger, and T.A. DeTemple, "Swept-Gain Superradiance in CO_2-Pumped CH_3F", this volume.

[10] This is a consequence of the relatively small value of T_2; the ringing is more effectively suppressed for $t_o = 2T_2$, as in this experiment, than it is for $t_o = 2T_2^*$, as shown in the calculations of Ref. 7 and those done by R. Saunders and R.K. Bullough, in Cooperative Effects in Matter and Radiation, C.M. Bowden, D.W. Howgate, and H.R. Robl, editors (Plenum, N.Y., 1977).

[11] E.A.J. Marcatili and R.A. Schmeltzer, Bell Syst. Tech. J., $\underline{43}$, 1783 (1964).

Table I. Experimental parameters for the case L = 3.5 m,
A $\simeq$ 11 cm^2, and p = .250 torr.

λ	496 μm
ρ	2.61×10^{13} cm^{-3}
N	1.01×10^{17}
$\alpha_o L$	125
ϕ_o	2.6×10^{-8}
$\|\ln \phi_o\|$	17.5
R_e	$-4.3 \ 10^{-3}$
L_c	53 cm
T_{sp}	229 sec
T_s	0.256 nsec
T_2	32 nsec
T_2^*	366 nsec

Above, ρ is the excited density and N = pAL the excited
number at pump cutoff, $\alpha_o L$ is the field gain per pass, R_e =
$(N_2 - N_1)e/N$ is the equilibrium population fraction, L_c =
$(8\pi^2 c T_{sp}/3\rho\lambda^2)^{1/2}$ is the cooperation length, and T_s =
$8\pi T_{sp}/\rho\lambda^2 L$ is the superradiant lifetime.

Table II. Sample comparison of experiment with theory for
the case L = 3.5 m, A $\simeq$ 11 cm^2.

p(torr)		t_o(nsec)	Δt(nsec)	I(W)
	Observed	125±6	41±5	6≠2
.123	Calculated (1)	109	49	10
	Calculated (2)	99	42	13
	Observed	62±5	22±3	24±8
.250	Calculated (1)	56	25	32
	Calculated (1)	53	23	38

(In this table, the delay t_o is measured from the vertical intercept of t_o vs. p^{-1} in Fig. 5 and is therefore an overestimate, as noted in the text).

Calculation (1): $\kappa = 2.15 \times 10^{-3} cm^{-1}$

$\phi_o(.123) = 2.3 \times 10^{-8}$

$\phi_o(.250) = 2.6 \times 10^{-8}$

Calculation (2): $\kappa = 3.00 \times 10^{-3} cm^{-1}$

$\phi_o(.123) = 6.2 \times 10^{-8}$

$\phi_o(.250) = 4.4 \times 10^{-8}$

Figure Captions

Fig. 1.   Partial energy level diagram for CH_3F pumped by a
CO_2 laser. The two fastest relaxation rates are
$\Gamma_J = 1.3 \times 10^8$ sec^{-1}torr^{-1} and $\Gamma_K = 1.2 \times 10^7$ sec^{-1}
torr^{-1}. The fractional populations in the initial
ground states, $f(J,K)$, are $f(12,1) = 6.89 \times 10^{-3}$,
$f(12,2) = 6.49 \times 10^{-3}$.

Fig. 2.   Experimental apparatus.

Fig. 3.   Typical pump (upper photo) and FIR pulses. All
scales are 50 nsec/division, and the displays are
synchronized.

Fig. 4.   Results for a sample with L = 4.7 m, A $\simeq$ 7 cm^2.
The straight lines are least-square fits to the data;
their slopes are pt_o = 17.7 nsec torr, $p\Delta t$ = 5.82
nsec-torr, I/p^2 = 421 W/torr^2. The homogeneously
broadened regime lies below p^{-1} = 12 torr^{-1}, or
above p^2 = 0.007 torr^2.

Fig. 5.   Results for samples with A = 11 cm^2, L = 3.5 and
2.3 m. The least-square slopes are pt_o(3.5m) = 15.4
nsec-torr, pt_0(2.3m) = 16.9 nsec-torr; $p\Delta t$(3.5m) =
5.08 nsec-torr, $p\Delta t$(2.3m) = 6.99 nsec-torr; I/p^2(3.5m) =
384 W/torr, I/p^2(2.3m) = 212 W/torr^2.
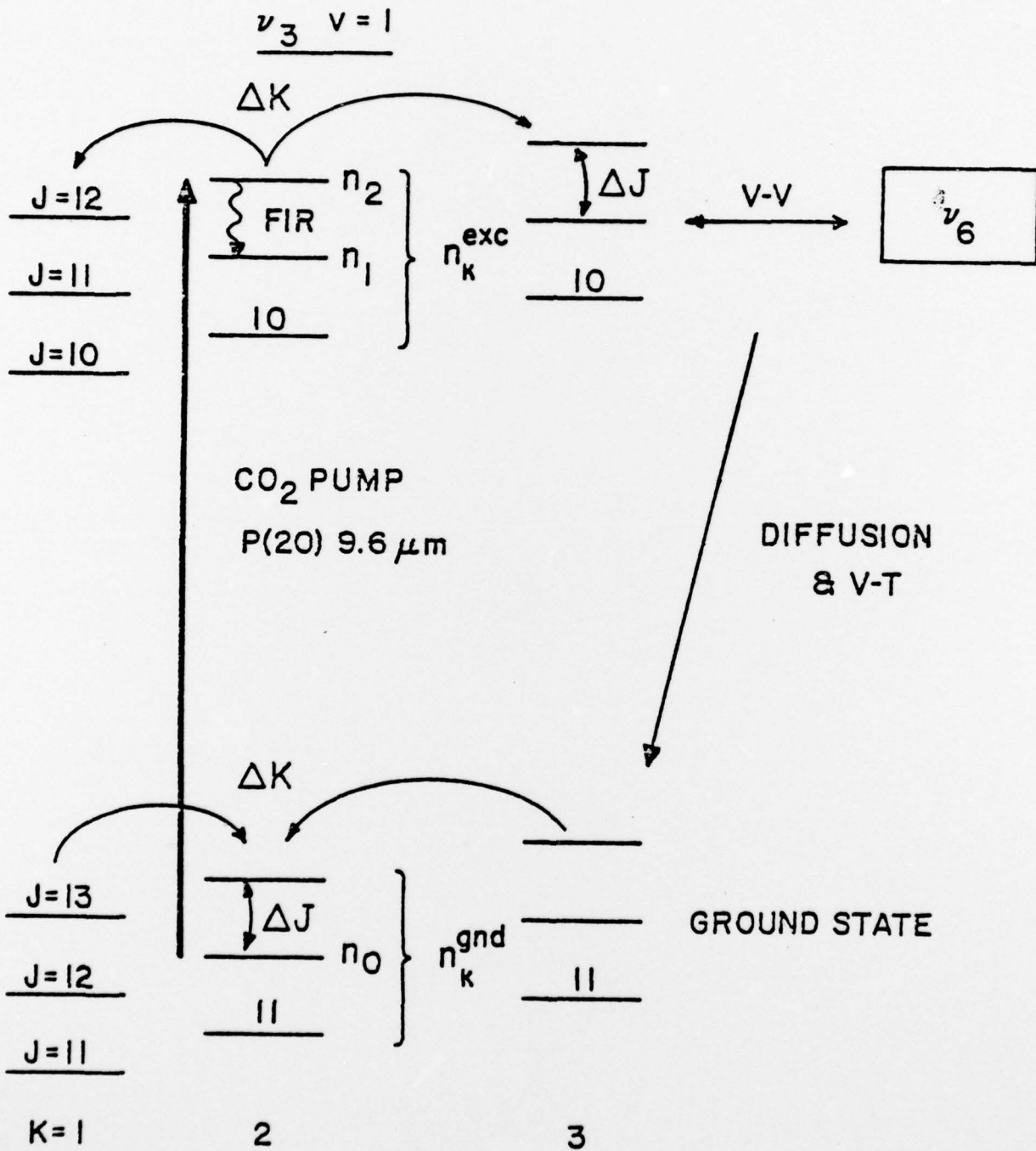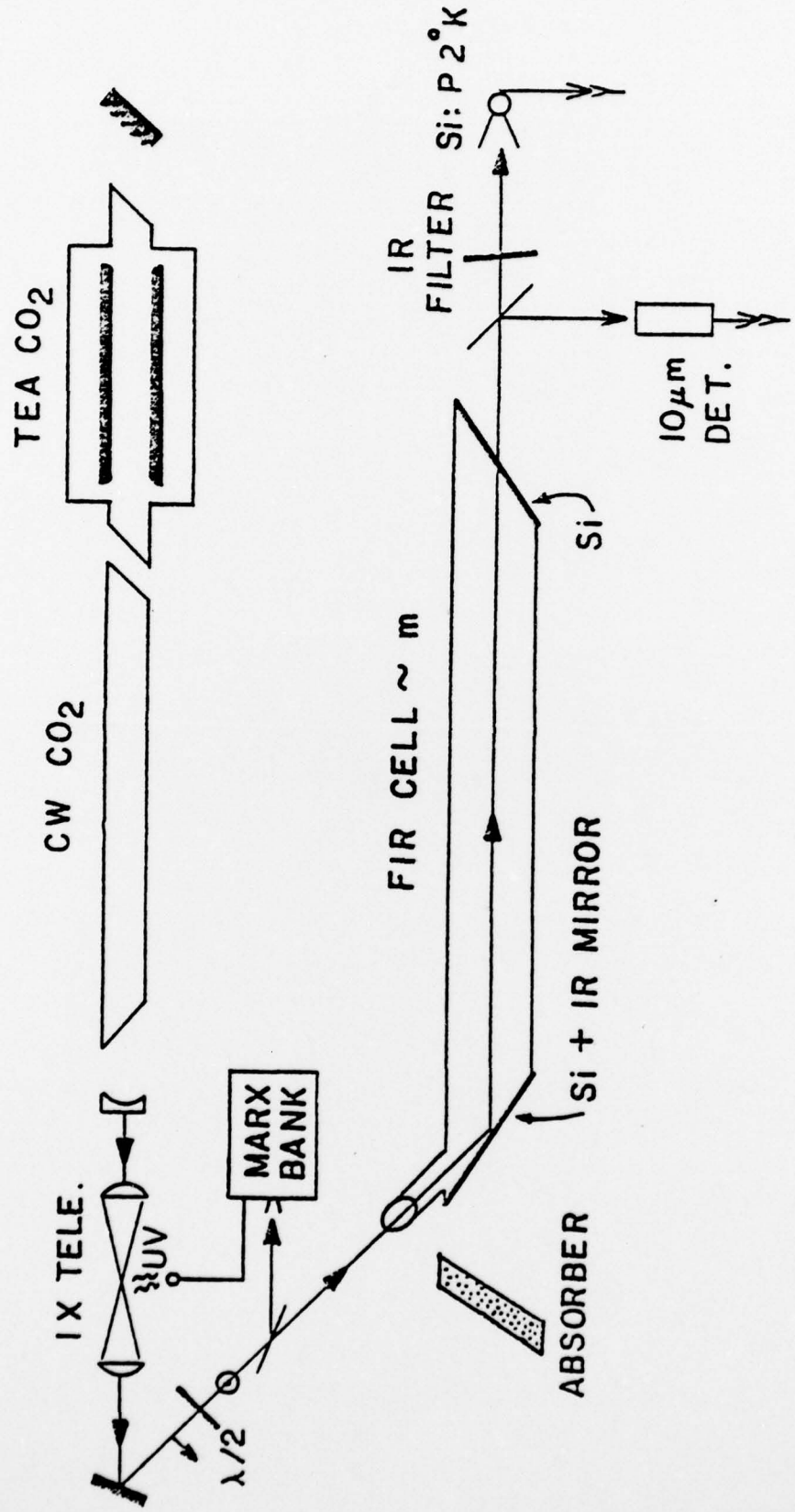
L = 2.3 m

9.6 μm CO_2

2 V
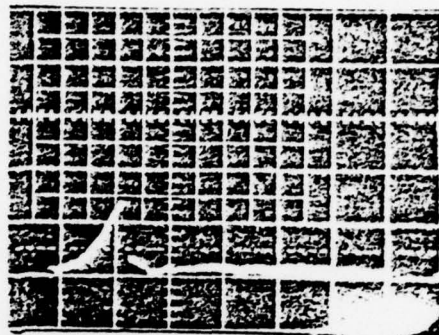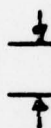
p = .320 torr
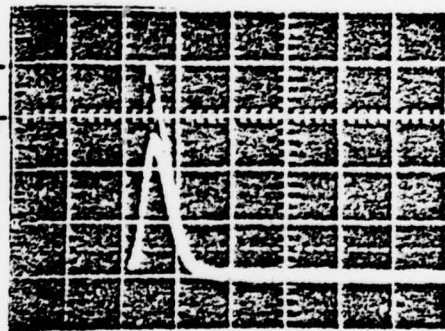
496 μm CH_3F

50 mV
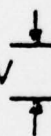
p = .133 torr
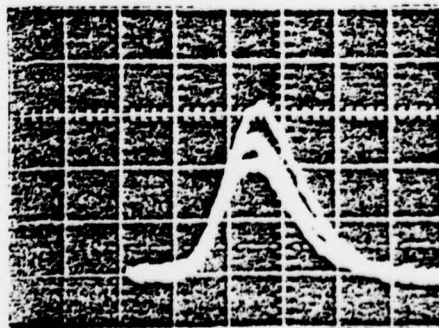
50 nsec
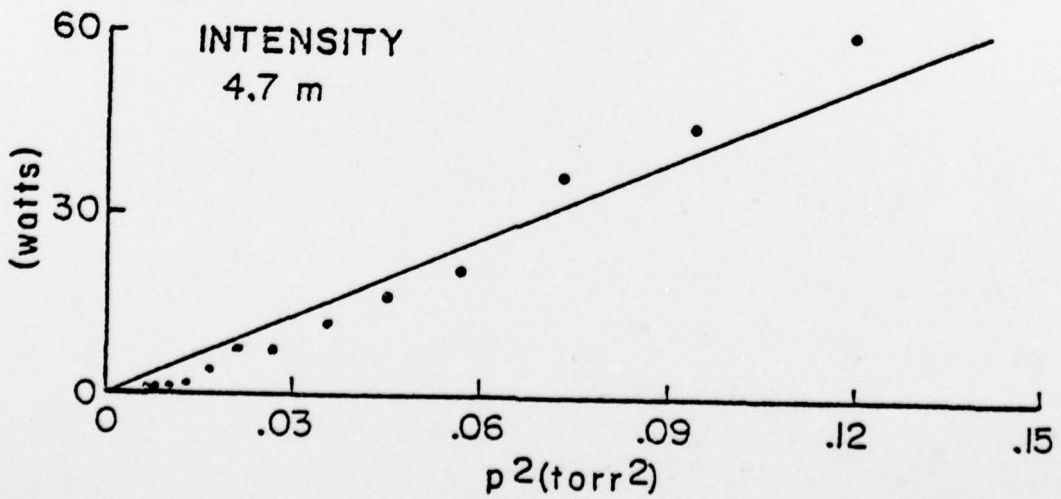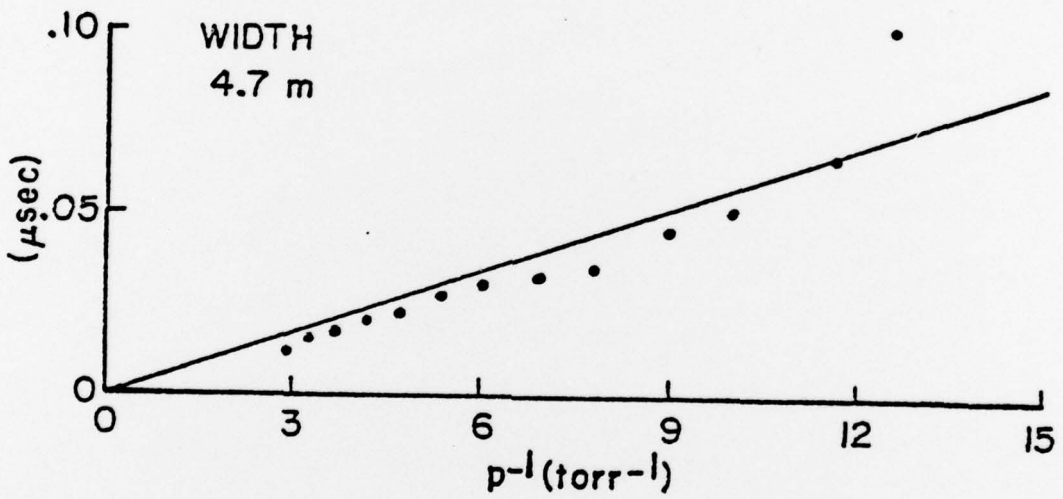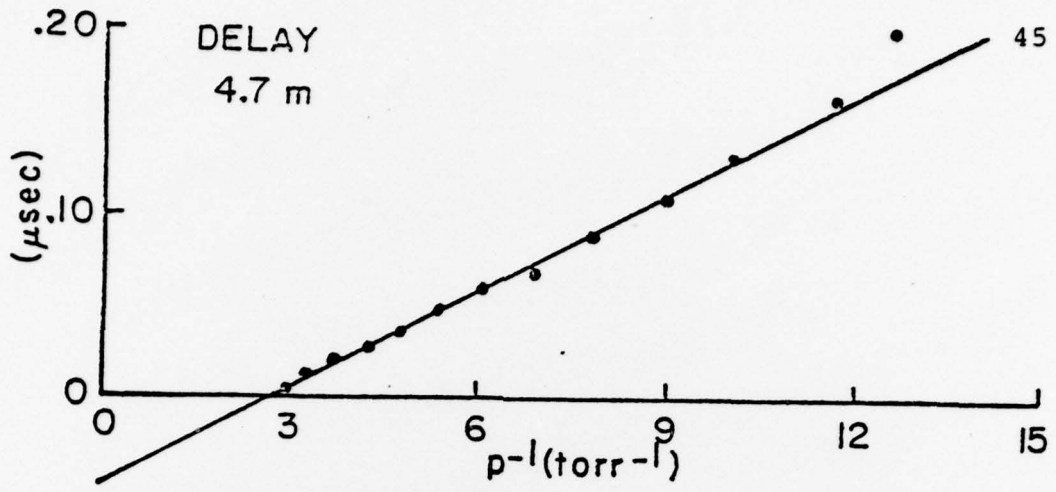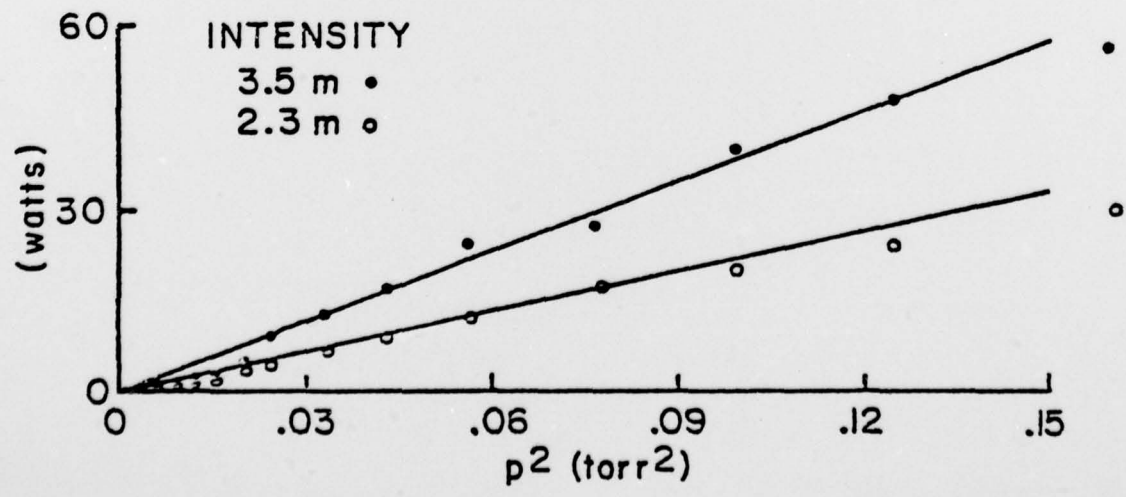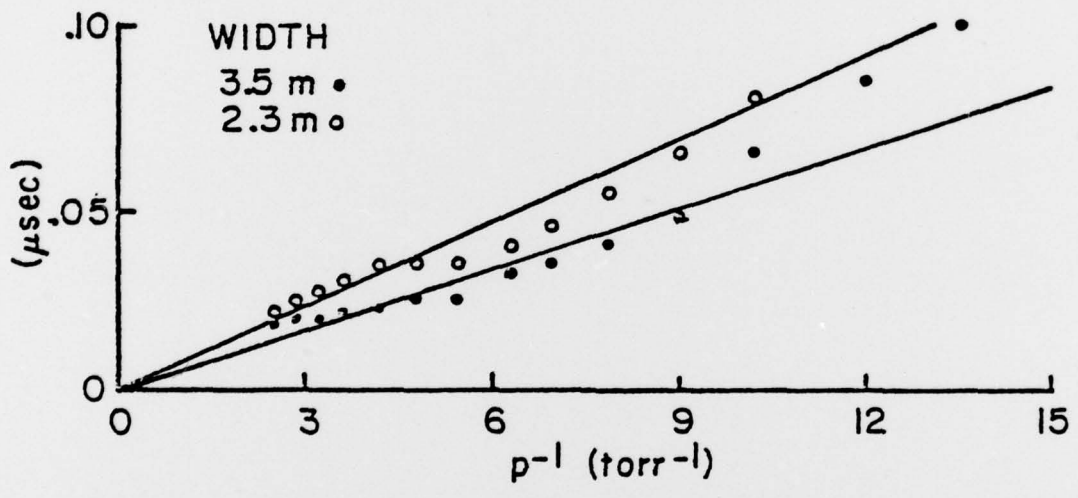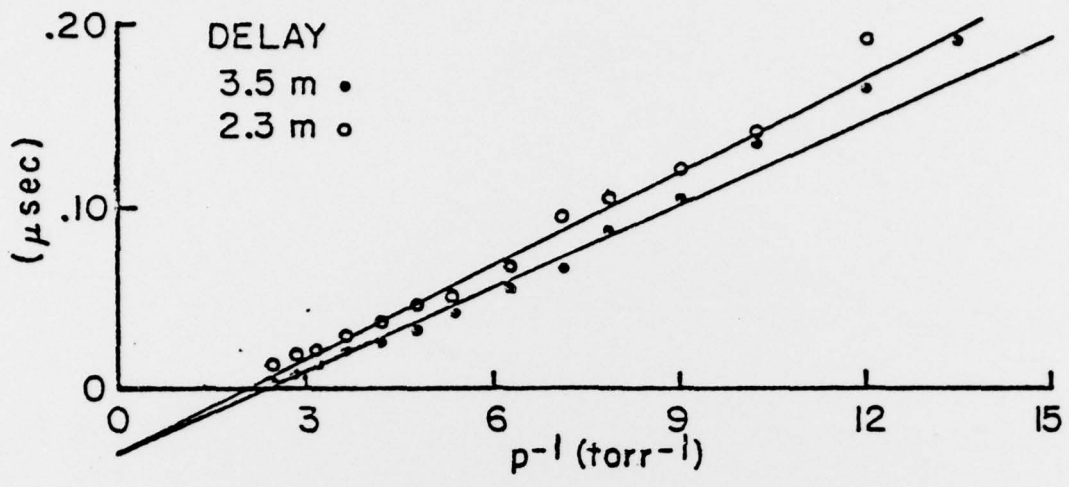
Stimulated Raman Emission in Infrared Excited Gases

S. J. PETUCHOWSKI, A. T. ROSENBERGER, AND THOMAS A. DeTEMPLE

Abstract—Using the pressure dependence of absorption, absorption coefficients and detunings were measured for CO_2 pump lines and the strong far infrared emission in optically pumped D_2O. The P (32) CO_2 line was found to be detuned ~1.5 GHz from the ν_2 band transitions 6_6, $6_5 \rightarrow 5_5$, 5_4. The resulting emission lines at 50.3 μm and 66 μm were found to be detuned from their respective transitions by about the same amount. On the basis of these measurements and gain estimates for the far infrared, the resulting emission lines are identified as stimulated Raman emission.

I. INTRODUCTION

INTEREST in far infrared (FIR) emission from optically pumped D_2O vapor stems from observations of high infrared to FIR conversion efficiency, ranking it along with $C^{12}H_3F$ as one of the stronger pulsed FIR sources [1]-[3]. Recent spectroscopic data have indicated that many of the pump lines are detuned many Doppler widths from their respective D_2O absorptions suggesting that off-resonant pumping is responsible for the strong emission [4]. Originally postulated to explain FIR emission in NH_3, off-resonant pumping is essentially wing absorption with resulting FIR emission on or near FIR line center [5]. An equally consistent and sometimes stronger off-resonant effect is stimulated Raman emission, which results in the FIR being emitted off-resonance by an amount equal to the pump detuning. In this article we present evidence for stimulated Raman emission in D_2O vapor.

In the next section, the experiment is discussed along with our recent spectral measurements and line identifications. In Section III, FIR frequency detuning measurements are presented along with Raman and laser gain estimates while the results are summarized in Section IV.

II. EXPERIMENT

In Fig. 1 is shown the experiment which was comprised of a CO_2 TEA laser, a 3.5 m long FIR cell, a grating monochromator, and an external absorption cell for wavelength and fine frequency measurements. The CO_2 laser operated on a single transverse and longitudinal mode, the latter obtained with the use of a CW low pressure CO_2 amplifier section. Using this technique the laser oscillated on CO_2 line center ±30 MHz

S. J. Petuchowski and A. T. Rosenberger are with the Department of Physics, University of Illinois, Urbana, IL 61801.
T. A. DeTemple is with the Department of Electrical Engineering, University of Illinois, Urbana, IL 61801.
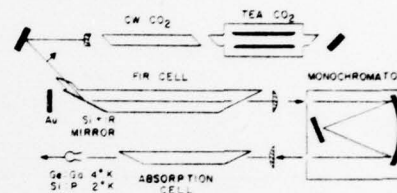

Fig. 1. Experimental arrangement. The absorption cell length was varied between 2 m and 20 cm.

with a single pulse spectral purity of better than 10 MHz including chirp [6].

The CO_2 pulse entered the FIR cell through a NaCl Brewster window and was reflected into the active region by a Si Brewster window. The interior portion of the Brewster window was coated with a multilayer Ge-ZnS IR mirror to provide >90 percent reflectivity throughout the CO_2 pump lines for the P-polarized pump [7]. This mirror had an estimated FIR absorption of <10 percent for wavelengths near 50 μm.

A single Au-coated flat was used as a back reflector while the output was transmitted either through another Si Brewster window or through a normal incidence high density polyethylene window. Most of the measurements were performed with the latter which implies a very low Q FIR cavity.

In view of the fact that there was only one line common to the previous two spectral measurements of the FIR emission from D_2O, we reanalyzed the spectral content associated with the strong emission using the P (32) 9.6 μm pump [1], [2]. This was performed with a $\frac{1}{2}$ m grating spectrometer using various FIR gratings in various orders and using higher orders of the weakly transmitted CO_2 as a wavelength marker. The accuracy of the measurements was ±0.1 μm with the results in basic agreement with previous observations [1].

Using the recent ν_2 band conventional spectroscopic measurements and resulting assignments of Shaw and Lin, we have been able to identify all IR and FIR transitions which are listed in Table I [4], [8]. The starred entries are new assignments. The notation is J_τ where $\tau = K_{-1} - K_{+1}$ and the strongly allowed transitions satisfy $\Delta J = 0$, ±1 and $\Delta \tau = 0$, ±2 [9].

A partial energy level diagram for the P (32) transition is shown in Fig. 2. Based on the results of Shaw and Lin, the insert shows the positions of the two transitions relative to
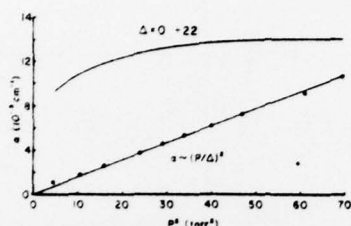
Fig. 4. Small signal absorption coefficient at P (32). Also shown is the line center absorption coefficient for I. Δ is the detuning from I.

TABLE II
MEASURED DETUNINGS

PUMP	α(/cm·torr^2)	$(\nu - \nu_0)$CALC^a	$\nu - \nu_0$ MEAS^c
P(32)	1.5×10^{-4}	+1.7 GHz (I)^b	$\leq$ 1.5 GHz
		-52 MHz (II)^b	$\leq$ 500 MHz
R(12)	1.4×10^{-4}	836 MHz	680 MHz
R(22)	1.8×10^{-3}	-81 MHz	318 MHz^d
R(32)	2.2×10^{-4}	773 MHz	670 MHz
R(34)	3.0×10^{-5}	-2.84 GHz	2.3 GHz

^{a}From Ref. 4

^{b}See Fig. 2

^{c}Assuming $\Delta\nu_H$ = 40 MHz/torr

^{d}From Ref. 2, also $\nu < \nu_0$ was determined

the detuning. Hence, a measured value of α versus p^2 can yield the detuning [12].

There are two major sources of error involved in applying this technique to frequency measurements. The first is in the broadening rates for individual transitions. From available data in H_2O and D_2O, the broadening rates range from 26-60 MHz/torr implying a detuning error of ±25 percent for an assumed average broadening rate of 40 MHz/torr [2], [13], [14]. The second source of error is in the possibility of absorption due to nearby transitions, which is correctable only to within the accuracy with which the spectra are known. From available sources we estimate the accuracies to be: ground state FIR, ±100 MHz, ν_2 IR, ±400 MHz, ν_2 FIR ±400 MHz [15]-[17].

Because of the known uncertainties of the IR transitions, particularly II in Fig. 2, and as a check on the technique, absorption coefficients and detunings were measured for a few CW pump lines listed in Table I [18]. An example of the data for P (32) is shown in Fig. 4. The results are presented in Table II with the detunings obtained using $\Delta\nu_H$ = 40 MHz/torr, a value based on our measured R (22) absorption coefficient and the known detuning of -318 MHz [2], [12]. These data essentially confirm the magnitude of the calculated detunings [4].

For the case of P (32), the analysis was complicated by the presence of the two transitions shown in Fig. 2. For two absorbing transitions there are generally four possible line locations which result in the same value of absorption. For the specific case of widely separated strong and weak transitions, the locations are approximately symmetric about each transition. For the data in Fig. 4, the resulting candidate line positions are ±855 MHz about I and ±500 MHz about II. But because of the linearity of α in Fig. 4 and the variation in α over the tuning range of the CW CO_2 laser we have deduced that the most likely line location is $\leq$ -500 MHz from II and $\leq$ +1.5 GHz from I [19]. Hence, the pump appears to be above the I line center by ~30 Doppler widths.

The technique was then applied to the FIR signals. Prior to propagating through the absorption cell, the intense (~kW) FIR pulses were filtered and attenuated to low levels (<W) to prevent saturation. The apparent absorption coefficient was then measured as a function of pressure in both the source and absorption cells with the resulting data shown in Fig. 5. Each data point represents an *energy* absorption coefficient

Fig. 5. (a) Measured FIR absorption coefficient for the 50 μm signal. Δ is the magnitude of the detuning from $6_{5,6} \rightarrow 7_{6,1}$. (b) Measured FIR absorption coefficient for the 66 μm signal. Δ is the magnitude of the detuning from ν_2 $4_{3,4} \rightarrow 5_{4,5}$. Also shown are line center absorption coefficients, and $\alpha(p^2)$ averaged over the experimental range of source cell pressures 1-5 torr.

averaged over ~100 FIR pulses. Part of the scatter is thus attributed to fluctuations in the pump and FIR amplitudes. As can be seen in this figure, the 50 μm signal appeared to be detuned 2.1 GHz, which is slightly greater than the estimated pump detuning of 1.5 GHz. The sign of the FIR detuning could not be determined.

For the 66 μm case, the absorption is dominated by the ground state transition $6_{-1} \rightarrow 7_1$ with a calculated location 5.75 GHz below the ν_2 FIR transitions. Because of the strong

PETUCHOWSKI *et al.*: STIMULATED RAMAN EMISSION

TABLE I
D₂O ASSIGNMENTS

PUMP[a]	ABS. (ν_2 BAND)	FIR(μm)	TRANSITION	
P(32)	*$6_{5,6} \rightarrow 5_{4,5}$	65.9 μm	*$4_{3,4} \rightarrow 5_{4,5}$	ν_2
		82.6 μm	$3_{2,3} \rightarrow 4_{3,4}$	ν_2
		50.3 μm	$6_{5,6} \rightarrow 7_{6,7}$	GND.
	$7_{-1} \rightarrow 6_{-3}$	119 μm	$5_{-3} \rightarrow 5_{-3}$	ν_2
R(12)	*$10_{-8} \rightarrow 9_{-6}$	94 μm	*$8_{-6} \rightarrow 9_{-6}$	ν_2
		114 μm	$9_{-8} \rightarrow 9_{-6}$	ν_2
		142 μm	*$10_{-8} \rightarrow 10_{-6}$	GND.
R(22)	$5_0 \rightarrow 4_0$	185 μm	$4_{-2} \rightarrow 4_0$	ν_2
		158 μm	$4_{-4} \rightarrow 4_{-2}$	ν_2
R(32)	$9_{-9} \rightarrow 8_{-7}$	116 μm	$7_{-7} \rightarrow 8_{-7}$	ν_2
R(34)	$4_2 \rightarrow 3_0$	263 μm	$3_{-2} \rightarrow 3_0$	ν_2

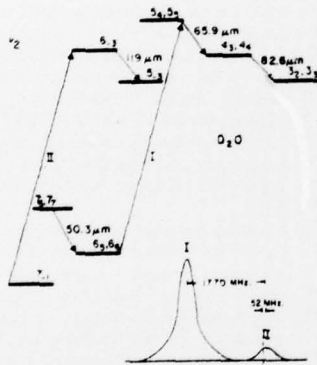[a]ν_2, 6 μm bands
*Newly Assigned

Fig. 2. Partial energy level diagram near the P(32) line. Insert shows the line positions and strengths based on conventional spectroscopic studies [4].

P(32) with the height being the relative absorption [4], [9]. The doublet transition from 6_5 and 6_6 is thought to be split by less than the Doppler width (50 MHz) [4]. Because the pump is essentially single frequency and detuned ~30 Doppler widths from the strongest absorption, the question arises as to the nature of the resulting FIR emission—laser or stimulated Raman. In what follows we present evidence that the 65.9 μm and the 50.3 μm transitions are due to stimulated Raman emission while the 82.6 μm appears to be a cascade laser transition. The 119 μm transition was not investigated.

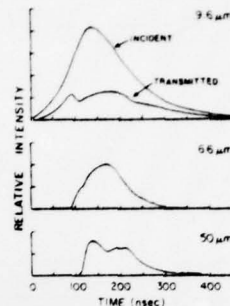Preliminary evidence for the Raman effect came from temporal measurements of the various signals shown in Fig. 3.

Fig. 3. Synchronized incident and transmitted CO_2 pulses, and emitted FIR pulses. Incident CO_2 ~ 0.6 MW, emitted FIR ~kW. The FIR detector was Si at 2 K with a speed of ~5 ns [10]. Source cell pressure: 3.4 torr.

Prior to the onset of the FIR, the CO_2 absorption coefficient was slightly less than the small signal value (to be discussed in the next section) indicating some small saturation. During the occurrence of the FIR, the peak absorption coefficient was a factor of 2 larger than the small signal value. This is incompatible with both FIR waves being on resonance because at best only the small signal absorption coefficient could be recovered by having saturating FIR waves present.

However, pump depletion and an apparent intensity dependent absorption coefficient are both characteristic of a strong parametric effect such as stimulated Raman emission. An alternate explanation of the increased absorption might be either a two-step or two-photon (IR + IR or IR + FIR) absorption. From the available spectroscopic data for ν_2, $2\nu_2$, ν_1, and ν_3, we have calculated that the smallest detuning for the latter processes is >10 GHz making the postulated Raman more favorable solely on the basis of detuning [4], [11].

III. DETUNING MEASUREMENTS

One of the major characteristics which distinguish the stimulated Raman signal from a laser signal is the optical frequency. In the latter case the frequency will be at the molecular frequency while in the former case, the frequency will be detuned from the molecular frequency by an amount equal to the pump detuning. In order to measure the expected small frequency shift, a second D_2O cell was used as a spectrometer, and is shown in Fig. 1.

For an assumed detuning much larger than the Doppler width, the wing absorption coefficient is given by

$$\alpha(\nu) = \frac{\lambda^2 A_{21}}{16\pi^2} \left(n_2 - \frac{g_2}{g_1} n_1 \right) \frac{\Delta\nu_H}{(\nu - \nu_0)^2} \qquad (1)$$

where 2 and 1 refer to the upper and lower levels, g_i is the level degeneracy, A_{21} is the reciprocal radiative lifetime, $\Delta\nu_H$ is the homogeneous line width (FWHM), and ν and ν_0 are the optical and molecular frequencies. Since both the population difference and the line width are proportional to pressure p, $\alpha \sim p^2$ with a slope inversely proportional to the square of

ground state transition, there are only two candidate line loca-
tions, +1.8 GHz and -6.75 GHz relative to the 66 μm line
center. The latter is rejected because it is inconsistent with
any Raman or laser process. The weak 83 μm signal was
absorbed strongly at all pressures and appeared to be on or
very near laser resonance. A consistent interpretation of
these results is that, by virtue of the measured IR and FIR
detunings, both the 50 and 66 μm signals are due to separate
stimulated Raman processes, with perhaps a small ac Stark
shift, while the 83 μm signal appears to be a cascade laser
transition. As a further check on this, we can estimate the
respective small signal gain coefficients and Stark shifts.

Using a density matrix description of two waves interacting
in a three-level system in the near-resonant approximation, the
gain at the emitted frequency can be expressed as

$$G_f \approx \pm\sigma_{32}\left[F_1(n_3 - n_2) + F_2(n_1 - n_2)\right] \qquad (2)$$

where the +(-) sign refers to the inverted (normal) vee con-
figuration shown in Fig. 6 and σ_{32} is the homogeneous cross-
section at line center for the $3 \rightarrow 2$ transition [20]. F_1 and
F_2 are the laser and Raman cross section multipliers, respec-
tively, with F_2 proportional to the pump intensity. The
explicit forms of F_1 and F_2 are listed in the Appendix. In
Fig. 6, F_1 and F_2 are shown versus the emitted frequency de-
tuning for a fixed pump detuning with normalized pump
intensity as a parameter. The values are representative of the
experimental situation in Fig. 3. Two key features to note
are that the laser and Raman resonances are ac Stark shifted
by the same amount in opposite directions and that the magni-
tude of F_2 is not negligible compared with F_1. For the in-
verted vee configuration appropriate to the 66 μm transition,
Raman gain exists for $n_1 > n_2$, which is certainly the case for
weak pump saturation. For the normal vee configuration
appropriate to the 50 μm transition, Raman gain requires $n_2 >
n_1$, which is also satisfied for a weak pump [21], [22].
Hence, both transitions may undergo separate laser or Raman
transitions.

The gain coefficients are estimated by approximating the
populations with a steady-state value. For the conditions in
Fig. 3 at the time of onset of the FIR, the Raman and laser
gains at 50 μm are found to be 0.5 cm^{-1} and -7 cm^{-1}, respec-
tively (assuming 1.5 GHz pump detuning, $\beta \approx 0.1$ correspond-
ing to ~300 kW/cm^2). For 66 μm the gains are estimated to
be 0.7 cm^{-1} and 0.5 cm^{-1} for the Raman and laser cases.
Because of the higher gain, the 66 μm Raman signal should
build up first followed by the 50 μm signal. This is evident in
Fig. 3.

Also evident in Fig. 3 is an inflection point in the 66 μm
signal which correlates with the onset of the 50 μm signal.
Considering the inverted vee configuration in Fig. 6, a 66 μm
Raman process results in a preferential population of 2 with
resulting wing absorption of the Raman signal due to the $2 \rightarrow 3$
transition. In contrast, a 50 μm Raman signal populates 3
which would decrease this absorption increasing the net 66 μm
Raman gain and resulting output as observed.

It is also interesting to note the predicted loss for the 50 μm
case. In fact even with a saturating pump and 66 μm signal,
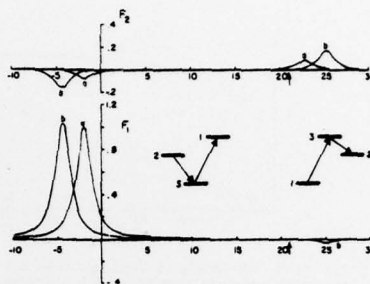laser or Raman, there is still a predicted 50 μm laser loss of

Fig. 6. Calculated values of F_1 and F_2 versus normalized FIR fre-
quency $2(r_{32} - r_f)/\Delta\nu_H$. Labels a and b refer to β values of 0.1 and
0.3, respectively, with β proportional to pump intensity as defined in
the Appendix. The arrows show the pump location. Insert shows
two possible Raman configurations.

-0.22 cm^{-1}. In contrast, the 66 μm laser and Raman gains
are very close, suggesting that other factors may influence the
preferential growth of one. One such factor is the ground
state absorption $6_{-1} \rightarrow 7_1$ which will be larger for the laser
case than the Raman, favoring the growth of the latter.

From Fig. 6, the ac Stark shift is estimated to be ~150
MHz assuming the detuning to be 1.5 GHz. Hence the Raman
lines should be detuned at least 1.65 GHz whereas any laser
lines would be detuned ~150 MHz. This is to be compared
with the measured 66 μm detuning of 1.8 GHz and the 50 μm
detuning of 2.1 GHz. Recalling the uncertainties in $\Delta\nu_H$,
the agreement is reasonable and confirms the nature of the
processes.

IV. CONCLUSIONS

Using the most recent high resolution spectral data, we have
identified the strong FIR transitions associated with the P(32)
pump. The expected pump detunings based on these data
have also been quantitatively confirmed. Because of the large
P(32) and emitted 50 and 66 μm signal detunings, the emis-
sion processes were identified as being due to two separate
stimulated Raman effects. The expected small ac Stark shift
of the FIR by the strong pump was not fully resolved. The
major error in using the pressure dependence of the absorption
for frequency measurements is in the uncertainties of the
various broadening coefficients.

There are a number of interesting implications of these
observations. First, a Raman process can be twice as efficient
as a laser process because, in principle, every absorbed IR
photon produces a Raman photon whereas laser emission is
limited to only half of the excited molecules. Second, the
strong-field near-resonant interaction produces an ac Stark
shift which, because of the space-time variation of the pump,
may chirp the FIR. In fact, the scatter evident in the data
of Fig. 5 has been partially correlated with the source cell
pressure and hence the FIR and IR intensities and their im-
plied Stark shifts. Third, the existence of absorption by
nearby ground state transitions may be a limiting factor in the
overall FIR growth dynamics. For example, the ground state

transition $4_{-4} \to 4_{-2}$, with a calculated position 3.68 GHz above the 385 μm transition, has a line center absorption of 0.45 cm^{-1} which may be sufficiently strong to affect the FIR. Finally, because of the presence of two strong FIR waves, there may exist contributions to the dynamics associated with three-photon processes such as a double Raman or laser-Raman process.

It would appear that under the appropriate tuning conditions, many of the multiphoton processes so easily observed in the visible may also be observed in the IR and FIR. Recent observations of two-photon absorption (IR + IR) and IR Raman, and this observation of FIR Raman, suggest that, far from being weak, the multiphoton effects are quite strong, may already exist in a number of known off-resonant cases, and might be observed in three- and four-wave interactions [5], [23]-[25].

APPENDIX

For times longer than the inverse linewidth, an appropriate rate equation description of the inverted vee configuration in Fig. 6 is

$$\dot{n}_2 = -\gamma_2 (n_2 - n_2^e) + G_f I_f$$
$$\dot{n}_1 = -\gamma_1 (n_1 - n_1^e) + G_p I_p$$
$$\dot{n}_3 = -\gamma_3 (n_3 - n_3^e) - G_p I_p - G_f I_f$$

where γ_i is the relaxation rate, n_i^e is the equilibrium population G is a gain coefficient, I_i the flux $\epsilon_0 E_i^2 / 2\hbar k_i$ with E_i the peak electric field and $k_i = 2\pi/\lambda_i$. The subscripts p and f refer to the pump and FIR. Using a density matrix description of a quasi steady-state two-wave interaction in the near resonant approximation (detunings are suboptical) and assuming all linewidths to be the same, the gain coefficients are found to be for the inverted vee case:

$$G_f = \sigma_{32} [(n_3 - n_2)F_1 + (n_1 - n_2)F_2]$$
$$G_p = \sigma_{31} [(n_1 - n_3)f_1 + (n_1 - n_2)f_2]$$

where σ_{ij} is the homogeneous cross section at line center [26]. Expressing detunings as $x = 2(\nu_{31} - \nu_p)/\Delta\nu_H$, $y = 2(\nu_{32} - \nu_f)/\Delta\nu_H$, normalized fields as $P = \mu_{13}E_p/\hbar\Delta\nu_H$ and $S = \mu_{23}E_f/\hbar\Delta\nu_H$ where μ_{ij} and ν_{ij} are the transition dipole moment and frequency; then defining $L(z) = z + i$, we find

$$F_1 = \mathrm{Im}\left(\left(1 + \frac{P^2 - S^2}{L(x-y)L(x)}\right) / L^*(y)\Delta \right)$$

$$F_2 = \mathrm{Im}\left(-P^2 / L(x-y)L(x)L^*(y)\Delta \right).$$

$$f_1 = \mathrm{Im}\left(\left(1 + \frac{P^2 - S^2}{L(x-y)L^*(y)}\right) / L(x)\Delta \right)$$

$$f_2 = -\sigma_{32} I_f F_2 / \sigma_{31} I_p$$

$$\Delta = 1 + P^2/L(x-y)L^*(y) - S^2/L(x-y)L(x).$$

These expressions contain ac Stark shifts due to *both* waves. In the weak field approximation $F_2 \simeq P^2/(x^2 + 1) = \beta$ at the Raman resonance ($y = x$). The data of Fig. 6 are for $S = 0$ and $\gamma_i = 2\pi\Delta\nu_H$.

REFERENCES

[1] D$_2$O was first suggested to us by F. Keilmann with the subsequent observation reported in: T. K. Plant, L. A. Newman, E. J. Danielewicz, T. A. DeTemple, and P. D. Coleman, "High power optically pumped far infrared lasers," *IEEE Trans. Microwave Theory Tech.*, vol. MTT-22, pp. 988-990, Dec. 1974.
[2] F. Keilmann, R. L. Sheffield, J. R. R. Leite, M. S. Feld, and A. Javan, "Optical pumping and tunable laser spectroscopy of the ν_2 band of D$_2$O," *Appl. Phys. Lett.*, vol. 26, pp. 19-22, Jan. 1, 1975.
[3] D. E. Evans, L. E. Sharp, W. A. Peebles, and G. Taylor, "Far-infrared super-radiant laser action in heavy water," *Opt. Commun.*, vol. 18, pp. 479-484, Sept. 1976.
[4] C. L. Lin and J. H. Shaw, "Measurements of ν_2 fundamental band of D$_2$ ^{16}O," presented at the 31st Symp. Molecular Spectroscopy, Columbus, OH, June 1976, paper FC10.
[5] H. R. Fetterman, H. R. Schlossberg, and J. Waldman, "Submillimeter lasers optically pumped off resonance," *Opt. Commun.*, vol. 6, pp. 156-159, Oct. 1972.
[6] R. I. Rudko, "Temporal coherence measurements of a double discharge CO$_2$ TEA laser," *IEEE J. Quantum Electron.*, vol. QE-11, p. 540, Sept. 1975.
[7] T. K. Plant and T. A. DeTemple, "Configurations for high-power pulsed CH$_3$F 496 μm lasers," *J. Appl. Phys.*, vol. 47, pp. 3042-3044, July 1976.
[8] J. Williamson, "ν_2 bands of H$_2$ ^{18}O, H$_2$ ^{16}O and D$_2$ ^{16}O," Ph.D. dissertation, Ohio State Univ., Columbus, 1969.
[9] A. L. Schawlow and C. H. Townes, *Microwave Spectroscopy*. New York: McGraw-Hill, 1955, ch. 4.
[10] P. Norton, "Photoconductivity from shallow negative donor loss in silicon: A new far-infrared detector," *J. Appl. Phys.*, vol. 47, pp. 308-320, Jan. 1976.
[11] W. S. Benedict, N. Gailar, and E. K. Plyer, "Rotation-vibration spectra of deuterated water vapor," *J. Chem. Phys.*, vol. 24, pp. 1139-1165, June 1956.
[12] Population differences and A coefficients can be calculated from the spectroscopic data, nuclear spin statistics, and asymmetric line strength data of [9]. The infrared A coefficients were calculated using a ν_2 band dipole moment of 0.12 D extrapolated from the measurements in [2].
[13] G. P. Srivastava and A. Kumar, "Foreign gas broadening by water molecule," *J. Chem. Phys.*, vol. 65, pp. 293-295, July 1, 1976.
[14] A value of 37 MHz/torr for the $6_{-4} \to 6_{-2}$ transition in D$_2$O was extrapolated from: C. C. Bradley, H. A. Gebbie, and W. J. Burroughs, "Observation of pressure broadening effects in D$_2$O using a CN maser," *Infrared Phys.*, vol. 7, pp. 129-134, Sept. 1967 and G. Duxbury and R. G. Jones, "High resolution submillimeter Stark spectroscopy using a CN maser," *Molecular Phys.*, vol. 20, pp. 721-734, Apr. 1971.
[15] G. Steenbeckeliers and J. Bellet, "Application of Watson's centrifugal distortion theory to water and light asymmetric tops. General methods. Analysis of the ground state and ν_2 state of D$_2$O^{16}," *J. Mol. Spectrosc.*, vol. 45, pp. 10-34, Jan. 1973.
[16] J. W. Fleming and M. J. Gibson, "Far-infrared absorption spectra of water vapor H$_2$ ^{16}O and isotopic modifications," *J. Mol. Spectrosc.*, vol. 62, pp. 326-337, Sept. 1976.
[17] The ground state estimate was obtained from comparison of measured FIR values in [16] with the predicted values from [15]. The ν_2 estimate was obtained by comparing the predicted IR $5_0 \to 4_0$ frequency with the measurement in [2] and by comparing predicted ground state FIR with the measurements of [15] and [16].
[18] To reduce possible absorption due to H$_2$O and HDO impurities, the absorption cell was repeatedly flushed with D$_2$O; in some cases the cell was heated to drive off the H$_2$O from the walls.
[19] The linearity enters because the correction term to (1) is nega-

tive and $\sim p^4$, thus enabling a minimum detuning from II to be set.

[20] The density matrix approach describing laser-Raman processes is discussed in: A. Javan, *Proceedings of the International School of Physics: Enrico Fermi*, vol. 31. New York: Academic, 1964, pp. 284-306; also K. Shimoda and T. Shimizu. *Progress in Quantum Electronics*, vol. 2, pt. 2. Oxford: Pergamon, 1972, sec. 2.2; also I. M. Beterov and V. P. Chebotaev, *Progress in Quantum Electronics*, vol. 3, pt. 1. Oxford: Pergamon, 1974, ch. IV.

[21] Raman effects from the vee configurations have been observed in He-Ne. A Schabert, R. Keil, and P. E. Toschek, "Dynamic Stark effect of an optical line observed by cross-saturation absorption," *Appl. Phys.*, vol. 6, pp. 181-184, Mar. 1975.

[22] For the stated inequalities, the FIR is a Stokes wave. Taking the opposite inequality results in FIR loss; the FIR would then be the pump and the IR the anti-Stokes.

[23] W. K. Bischel, P. J. Kelley, and C. K. Rhodes, "Observation of Doppler-free two photon absorption in the ν_3 bands of CH_3F." *Phys. Rev. Lett.*, vol. 34, pp. 300-303, Feb. 10, 1975. R. R. Jacobs, D. Prosnitz, W. K. Bischel, and C. K. Rhodes, "Laser generation from 6 to 35 μm following two-photon excitation of ammonia," *Appl. Phys. Lett.*, vol. 29, pp. 710-712, Dec. 1, 1976.

[24] E. J. Danielewicz, E. G. Malk, and P. D. Coleman, "High-power vibration-rotation emission from $^{14}NH_3$ optically pumped off resonance," *Appl. Phys. Lett.*, vol. 29, pp. 557-559. Nov. 1, 1976. T. Y. Chang and J. D. McGee, "Off-resonant infrared laser action in NH_3 and C_2H_4 without population inversion." *Appl. Phys. Lett.*, vol. 29, pp. 725-727, Dec. 1, 1976.

[25] S. Petuchowski, J. Oberstar, and T. A. DeTemple, unpublished.

[26] Degeneracy effects have been neglected in these equations and are treated in: Yu. A. Il'inskii and R. Y. Khokhlov, "Theory of stimulated Raman scattering by rotational transitions," *Sov. Phys. -JETP*, vol. 37, pp. 619-621, Oct. 1973.